Journal of Medicinal Chemistry

ARTICLE

pubs.acs.org/jmc

From Fragment Screening to In Vivo Efficacy: Optimization of a Series of 2-Aminoquinolines as Potent Inhibitors of Beta-Site Amyloid Precursor Protein Cleaving Enzyme 1 (BACE1)†

Yuan Cheng,*,‡ Ted C. Judd,*,‡ Michael D. Bartberger,§ James Brown,‡ Kui Chen,⊥ Robert T. Fremeau, Jr.,∥ Dean Hickman,# Stephen A. Hitchcock,▽ Brad Jordan,§ Vivian Li,§ Patricia Lopez,‡ Steven W. Louie,# Yi Luo,∥ Klaus Michelsen,§ Thomas Nixey,‡ Timothy S. Powers,‡ Claire Rattan,∥ E. Allen Sickmier,§ David J. St. Jean, Jr.,‡ Robert C. Wahl,⊥ Paul H. Wen,∥ and Stephen Wood∥

‡Chemistry Research and Discovery, §Department of Molecular Structure, ∥Department of Neuroscience, ⊥Department of HTS and Molecular Pharmacology, #Department of Pharmacokinetics and Drug Metabolism, Amgen Inc., One Amgen Center Drive, Thousand Oaks, California 91320, United States

Supporting Information

ABSTRACT: Using fragment-based screening of a focused fragment library, 2-aminoquinoline **1** was identified as an initial hit for BACE1. Further SAR development was supported by X-ray structures of BACE1 cocrystallized with various ligands and molecular modeling studies to expedite the discovery of potent compounds. These strategies enabled us to integrate the C-3 side chain on 2-aminoquinoline **1** extending deep into the P2′ binding pocket of BACE1 and enhancing the ligand's potency. We were able to improve the BACE1 potency to subnanomolar range, over 10^6-fold more potent than the initial hit (900 μM). Further elaboration of the physical properties of the lead compounds to those more consistent with good blood−brain barrier permeability led to inhibitors with greatly improved cellular activity and permeability. Compound **59** showed an IC_{50} value of 11 nM on BACE1 and cellular activity of 80 nM. This compound was advanced into rat pharmacokinetic and pharmacodynamic studies and demonstrated significant reduction of Aβ levels in cerebrospinal fluid (CSF).

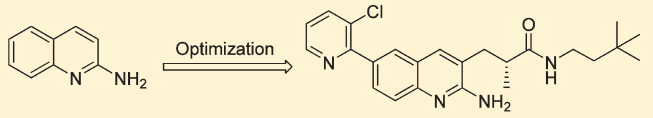

1 BACE1 K_d = 900 μM

59 BACE1 IC_{50} = 0.011 nM

INTRODUCTION

Alzheimer's disease (AD) is a progressive neurological disease of the brain that leads to the irreversible loss of neurons and dementia. The clinical hallmarks of AD include progressive impairment in memory, judgment, decision making, orientation to physical surroundings, and language. Current standards of care including the acetylcholinesterase inhibitors and NMDA receptor antagonists provide temporary symptomatic relief but do not alter the underlying disease pathophysiology. A therapeutic treatment that directly modifies the progression of the disease remains one of the largest unmet medical needs.

The pathological hallmarks of AD include the deposition of amyloid β (Aβ) in the neural parenchyma and the formation of neuronal tangles. The study of disease genes that are associated with familial cases of AD has implicated the accumulation of the Aβ peptide as a key early initiating event in the pathogenesis of this disorder.[1] The genetic findings form the basis for the amyloid hypothesis of AD, which suggests that accumulation of the Aβ peptide in toxic protein aggregates due to an imbalance between production and clearance triggers numerous pathophysiological changes that ultimately lead to synaptic failure, neurodegeneration, and cognitive dysfunction.[2] Aβ is produced by the sequential endoproteolytic cleavage of amyloid precursor protein (APP) by two proteases, the β- and γ-secretases.[3,4] β-Secretase cuts APP first to generate the amino terminus of Aβ, producing soluble amyloid precursor protein-β (sAPPβ) and a membrane bound C-terminal fragment called C99. γ-Secretase then cleaves C99 to release the mature Aβ peptide. Inhibition of β-secretase decreases the production of all forms of Aβ, including the most pathogenic species, $A\beta_{42}$[5] indicating that β-secretase is a prime therapeutic target for the development of disease-modifying therapies for AD.[6]

In 1999, β-secretase was identified as the type 1 transmembrane aspartyl protease BACE1 that is related to the pepsin and retroviral aspartic protease families.[3] The highest levels of BACE1 expression are found in neurons in the brain.[3] BACE1 $^{-/-}$ mice are viable, fertile, and do not produce cerebral Aβ.[7] Furthermore, when BACE1 $^{-/-}$ mice are crossed with APP transgenic mice that overexpress mutant APP, the deficiency in BACE1 activity rescues the amyloid pathology and synaptic and behavioral dysfunction observed in the APP transgenic mice.[8] These results indicate that BACE1 is essential for producing amyloidogenic Aβ peptides in the mammalian brain.

BACE1 is located in the central nervous system (CNS) and characterized by a large binding site to recognize 6−8 amino acid

Received: May 3, 2011
Published: June 27, 2011

residues of APP. There are significant challenges in designing low-molecular-weight, brain penetrant, potent BACE1 inhibitors.[9] Traditional high throughput screening (HTS) methods have met with very limited success, and most lead compounds have been derived by rational structure-based design of peptidomimetics.[10−13] The majority of these compounds possess a secondary alcohol as a transition state mimetic that displaces an active-site water molecule and forms hydrogen bonding interactions with the catalytic aspartates. Although some of the initial peptidomimetic inhibitors were very potent in vitro, these inhibitors tended to have multiple hydrogen bond donors and acceptors along with relatively high molecular weight (MW > 500). These characteristics present challenges to further development of these compounds into CNS penetrable BACE1 inhibitors devoid of P-glycoprotein (Pgp) mediated efflux liabilities.[14,15] As such, a majority of these peptidomimetic inhibitors were not able to demonstrate significant CNS Aβ lowering in rodent pharmacodynamic (PD) models. In recent years, there has been a growing interest from a number of groups focused on developing nonpeptidomimetic BACE1 inhibitors.[15−18] However, only a few compounds in this class are known in the literature to show both good in vitro potency (in the low nanomolar range) and also demonstrate significant Aβ reduction in CNS. Therefore, identification of nonpeptidic small molecule BACE1 inhibitors that are both highly potent and CNS penetrable remains a major challenge.

In an effort to identify nonpeptidic leads with the potential for desired CNS penetration, we employed a fragment-based screening approach. Fragment-based screening has become a valuable alternative to traditional HTS screening, offering the possibility of identifying novel leads with much lower molecular weight than those generated from HTS.[19−22] Fragment-based hits are typically small (MW 150−250) and have weak affinity (K_d ∼ 100−2000 μM) but high ligand efficiency (LE).[22−25] Optimization of fragment hits guided by LE and physical properties can provide opportunities to design lead compounds with the desired drug-like properties. However, fragment-based screening can be challenging in practice as robust detection techniques are necessary to detect low affinity compounds. Ideally, having more than one screening method is desirable in order to confirm the on-mechanism activity of fragment hits and minimize the number of compounds that give false positive results. In practice, access to cocrystal structures of the target and fragment hits is also crucial for further confirmation and optimizations of the hits. Because these requirements were able to be satisfied with the BACE1 enzyme target, the fragment-based screening approach appeared to be an appealing strategy.

There have been reports in recent years demonstrating the success of fragment-based screening approach on BACE1[17,26−31] and several fragment hits inhibiting BACE1 with good LE having been identified. However, few of these inhibitors developed from fragment-based screening were reported to reduce Aβ peptide production in the CNS.

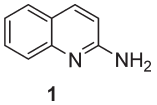

1

Figure 1. 2-Aminoquinoline as an initial fragment hit capable of inhibiting BACE.

Our efforts implementing fragment-based screening to identify potent BACE1 inhibitors have led to a class of aminoquinolines that are highly potent and brain penetrable. Starting with a focused fragment library that was screened using surface plasmon resonance (SPR) based technology,[32] one of the initial fragment hits, 2-aminoquinoline **1**, displayed potency in the millimolar range with excellent LE (Figure 1). 2-Aminoquinoline **1** has been reported in the literature as a weak inhibitor of BACE1 along with its cocrystal structure revealing its mode of binding.[30,31] On the basis of the high ligand efficiency of **1** and the existence of structural information regarding its binding, this fragment was selected as one of the more promising starting points for further optimization.

Development of **1** was by supported by X-ray determination of key BACE1 cocrystal structures along the optimization pathway in conjunction with modeling studies, expediting the discovery of compounds with increasingly greater affinity. Close attention was paid to the physical properties of the lead compounds, giving rise to inhibitors with favorable cellular activity and permeability. The optimized aminoquinoline BACE1 inhibitor **59** was evaluated in rat pharmacodynamic studies and demonstrated significant CSF Aβ reduction. The evolution of the structure−activity relationship, as well as optimization of physical properties conducive to blood−brain barrier penetration, will be the central focus of this report.

CHEMISTRY

The synthesis of bromo-substituted 2-aminoquinoline analogues as shown in Table 1 is summarized in Scheme 1. Commercially available bromo-substituted quinolin-2(1*H*)-ones (**2**) was refluxed with phosphorus oxychloride to give 2-chloroquinoline **3**. The chlorine displacement with 4-methoxybenzylamine followed by removal of the 4-methoxylbenzyl group using trifluoroacetic acid afforded bromo-substituted 2-aminoquinolines **28**−**31**.

6-Substituted 2-aminoquinoline analogues **32**−**38** shown in Table 2 were prepared from Suzuki coupling of boronic acids with 6-bromo-2-aminoquinoline **4** (Scheme 2). 6-(2-(3,3-Dimethylbut-1-ynyl)phenyl)quinolin-2-amine **39** was prepared from 6-aminoquinoline **5** by converting the amino group to

Scheme 1. Synthesis of Bromo-Substituted 2-Aminoquinoline Derivatives[a]

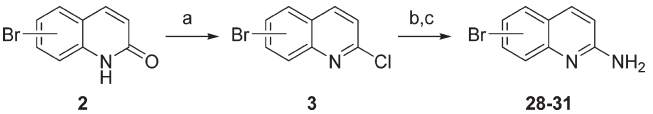

2 3 28-31

[a] Reagents and conditions: (a) phosphorus oxychloride, reflux; (b) 4-methoxybenzylamine, *N*-methylpyrrolidinone, 140 °C; (c) trifluoroacetic acid, 60 °C.

Scheme 2. Synthesis of 6-Substituted 2-Aminoquinoline Derivatives[a]

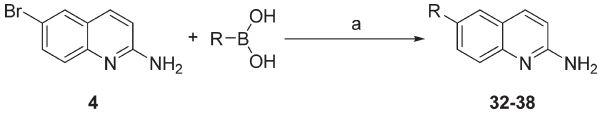

4 32-38

[a] Reagents and conditions: (a) potassium carbonate, PS (polystyrene)-triphenylphosphine palladium(0), dimethoxyethane/ethanol, microwave, 140 °C, 10 min.

dx.doi.org/10.1021/jm200544q | *J. Med. Chem.* 2011, 54, 5836–5857

Scheme 3. Synthesis of 6-(2-(3,3-Dimethylbut-1-ynyl)phenyl)quinolin-2-amine[a]

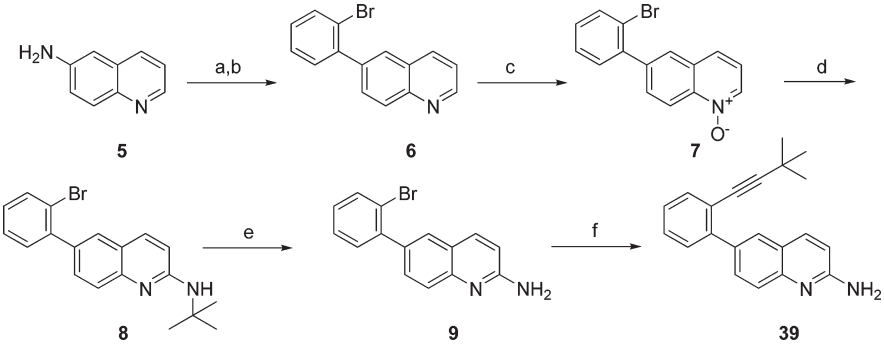

[a] Reagents and conditions: (a) $NaNO_2$, HCl, NaI, ethyl acetate; (b) 2-bromophenylboronic acid, potassium carbonate, tetrakistriphenylphosphine palladium(0), ethanol, reflux; (c) *m*-chloroperoxybenzoic acid, chloroform, reflux; (d) trifluoromethylbenzene, *tert*-butylamine, *p*-toluenesulfonic anhydride, 25 °C; (e) trifluoroacetic acid, 80 °C; (f) triethylamine, copper(I) iodide, dichlorobis(triphenylphosphine)palladium(II), 4,4-dimethylpent-2-yne, dimethylformamide, 140 °C.

Scheme 4. Synthesis of 3-Substituted 2-Aminoquinoline Derivatives[a]

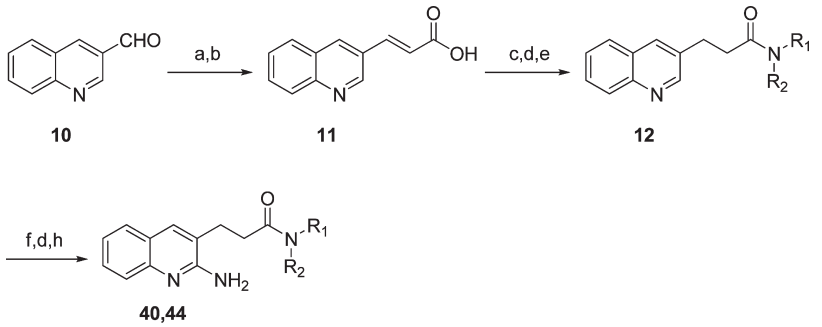

[a] Reagents and conditions: (a) methyl-(triphenylphosphoranylidene)-acetate, THF, 60 °C; (b) lithium hydroxide, methanol/H_2O, 50 °C; (c) thionyl chloride, 80 °C; (d) *N*,*N*-diisopropylethylamine, R_1R_2NH, dichloromethane, 25 °C; (e) H_2, Pd/C, methanol; (f) *m*-chloroperoxybenzoic acid, chloroform, reflux; (g) trifluoromethylbenzene, *tert*-butylamine, *p*-toluenesulfonic anhydride, 25 °C; (h) trifluoroacetic acid, 80 °C.

Scheme 5. Synthesis of 6-Aryl C-3 Substituted 2-Aminoquinoline Derivatives[a]

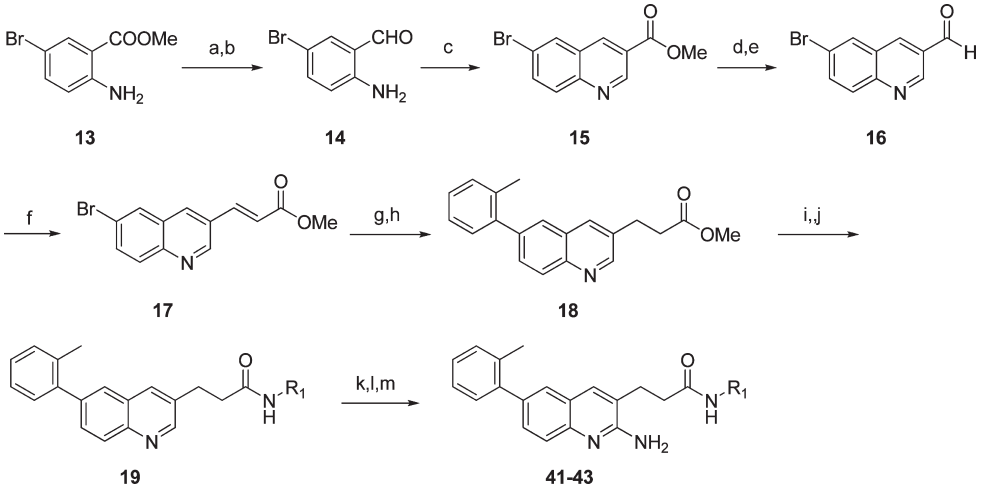

[a] Reagents and conditions: (a) lithium aluminum hydride, THF, −78 °C; (b) manganese dioxide, dichloromethane; (c) methyl 3,3-dimethoxypropionate, toluenesulfonic acid, toluene, 140 °C; (d) diisobutylaluminum hydride, dichloromethane, −78 °C; (e) Dess−Martin periodinane, dichloromethane; (f) methyl (triphenylphosphoranylidene) acetate, THF, 70 °C; (g) *o*-tolylboronic acid, potassium acetate, bis(4-(di-*tert*-butylphosphino)-*N*,*N*-dimethylbenzenamine) dichloropalladium(II), water, ethanol, reflux; (h) H_2, Pd/C, ethanol; (i) LiOH, methanol, 50 °C; (j) thionyl chloride, 80 °C, then R_1NH_2, or R_1R_2NH, *N*,*N*-diisopropylethylamine, dichloromethane; (k) *m*-chloroperoxybenzoic acid, chloroform, reflux; (l) trifluoromethylbenzene, *tert*-butylamine, *p*-toluenesulfonic anhydride, 25 °C; (m) trifluoroacetic acid, 80 °C.

dx.doi.org/10.1021/jm200544q |*J. Med. Chem.* 2011, 54, 5836–5857

Scheme 6. Synthesis of α-Substituted Amide Intermediates[a]

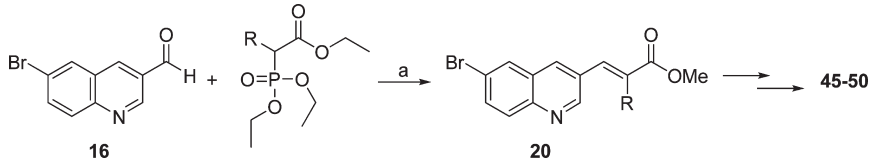

[a] Reagents and conditions: (a) potassium *tert*-butoxide, THF, 25 °C.

Scheme 7. Synthesis of 6-*o*-Tolyl 2-Aminoquinoline Amide Derivatives[a]

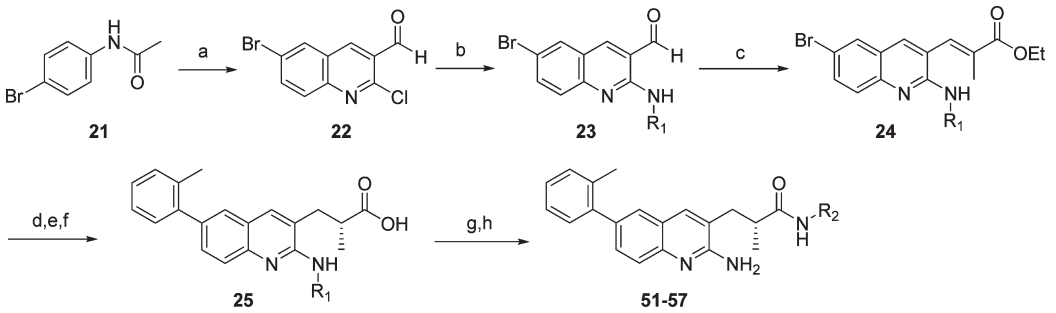

[a] Reagents and conditions: (a) phosphorus oxychloride, DMF, 75 °C; (b) 4-methoxybenzylamine, NMP, 130 °C or *tert*-butylamine, ethanol, 125 °C; (c) ethyl 2-(diethoxyphosphoryl)propanoate, lithium chloride, acetonitrile, 25 °C; (d) *o*-tolylboronic acid, potassium acetate, bis(4-(di-*tert*-butylphosphino)-*N*,*N*-dimethylbenzenamine) dichloropalladium(II), water, ethanol, reflux; (e) H_2, Pt/C, ethanol; (f) LiOH, methanol/THF; (g) *O*-(benzotriazol-1-yl)-*N*,*N*,*N*′,*N*′-tetramethyluronium tetrafluoroborate, R_2NH_2, *N*,*N*-diisopropylethylamine, NMP; (h) trifluoroacetic acid, 80 °C.

Scheme 8. Synthesis of 6-Substituted 2-Aminoquinoline 3,3-Dimethylbutanyl Amide Derivatives[a]

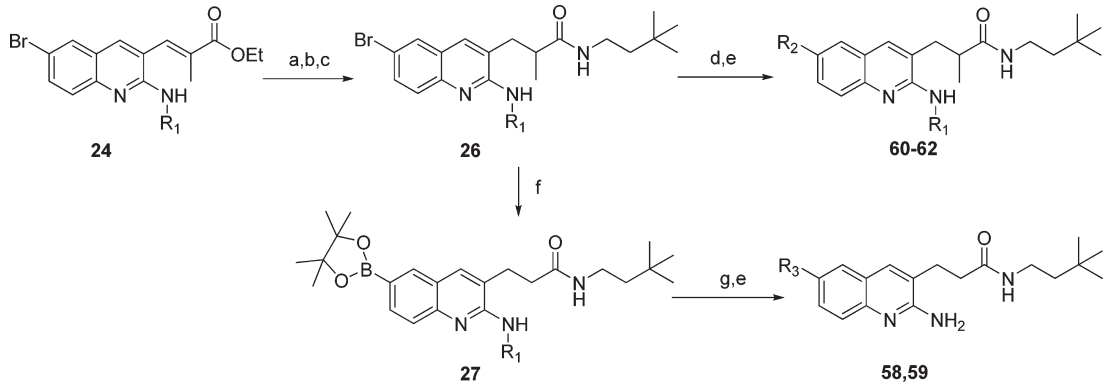

[a] Reagents and conditions: (a) LiOH, methanol/THF; (b) H_2, Pt/C, ethanol. (b) *O*-(benzotriazol-1-yl)-*N*,*N*,*N*′,*N*′-tetramethyluronium tetrafluoroborate, 3,3-dimethylbutanamine, *N*,*N*-diisopropylethylamine, NMP; (c) H_2, Pt/C, ethanol; (d) R_2-boronic acid, potassium acetate, bis(4-(di-*tert*-butylphosphino)-*N*,*N*-dimethylbenzenamine) dichloropalladium(II), water, ethanol, reflux; (e) trifluoroacetic acid, 80 °C; (f) dichloro(1,1′-bis(diphenylphosphino)ferrocene) palladium(II), potassium acetate, 4,4,5,5-tetramethyl-2-(4,4,5,5-tetramethyl-1,3,2-dioxaborolan-2-yl)-1,3,2-dioxaborolane, dioxane, 85 °C; (g) R_3Br, potassium acetate, bis(4-(di-*tert*-butylphosphino)-*N*,*N*-dimethylbenzenamine) dichloropalladium(II), water, ethanol, reflux.

the iodide followed by Suzuki coupling with 2-bromophenylboronic acid to give 6-(2-bromophenyl)quinoline **6** (Scheme 3). The 2-amino group was installed by formation of the quinoline *N*-oxide **7** by oxidation with *m*-chloroperoxybenzoic acid and then treatment with toluenesulfonic anhydride and *tert*-butylamine in trifluoromethylbenzene to afford the corresponding the *tert*-butylamine derivative **8**. Removal of the *tert*-butyl group under acidic conditions gave the free 2-amino analogue 6-(2-bromophenyl)quinolin-2-amine **9**. Palladium catalyzed coupling of **9** with 4,4-dimethylpent-2-yne afforded 6-(2-(3,3-dimethylbut-1-ynyl)phenyl)quinolin-2-amine **39**.

The synthesis of 3-substituted 2-aminoquinoline analogues in Table 3 started with commercial available quinoline-3-aldehyde **10**, which was converted to methyl 3-(quinolin-3-yl)acrylate by Wittig olefination with methyl-(triphenylphosphoranylidene)-acetate (Scheme 4). Hydrolysis of the ester group gave the acid **11** and amide formation followed by hydrogenation of the olefin provided the amide **12**. The 2-amino group was installed as previously described in the preparation of **39** in Scheme 3 to give the 2-amino analogues **40** and **44**.

Scheme 5 describes the synthesis of 6-*o*-tolyl 3-substituted 2-aminoquinoline analogues that are shown in Table 3. The

dx.doi.org/10.1021/jm200544q |*J. Med. Chem.* 2011, 54, 5836–5857

methyl ester of **13** was converted to the aldehyde **14** by reduction with lithium aluminum hydride followed by oxidation with manganese dioxide. Heating of **14** with methyl 3,3-dimethoxypropionate and catalytic toluenesulfonic acid in toluene afforded methyl 6-bromoquinoline-3-carboxylate **15**. The ester group of **15** was converted to the aldehyde **16**, which underwent a Witting olefination with methyl (triphenylphosphoranylidene) acetate to give **17**. Suzuki coupling with *o*-tolylboronic acid, followed by hydrogenation of the olefin, provided **18**. Hydrolysis of the methyl ester and amide coupling with various amines afforded **19**. The 2-amino group was installed as described in Scheme 3 to give compound **41**−**43**.

The compounds with substitution at the α-position of the amide in Table 4 were prepared in an analogous manner as described in Scheme 6, except the C-3 linker was installed with the aldehyde **16** by Horner−Wadsworth−Emmons reaction with various substituted phosphonate esters to give **20**. **45**−**50** were prepared by the same procedures (**17** to **41**−**43**) as described in Scheme 5.

Alternatively, α-methyl amide analogues as shown in Scheme 7 could be synthesized from the 3-aldehyde quinoline **22** prepared in one step via Vilsmeier reaction using a modified procedure from the literature[33] and functionalization at the 2-position. Compounds in Table 5 were prepared using this method. Thus *N*-(4-bromophenyl)acetamide **21** was treated with phosphorus oxychloride and DMF to give 2-chloroquinoline aldehyde **22**. The chlorine atom was displaced by 4-methoxybenzylamine or *tert*-butylamine to afford **23**. Horner−Wadsworth−Emmons olefination on aldehyde **23** with ethyl 2-(diethoxyphosphoryl)-propanoate gave the common intermediate ester **24**, which was further modified by both amide replacement of the ester and 6-bromo substitution to access the final compounds. Suzuki coupling between the *o*-tolylboronic acid, followed by hydrolysis of the ester group and hydrogenation of the olefin, afforded the acid **25**. At this stage, the (*R*)-enantiomer could be isolated by chiral HPLC separation. The acid **25** was coupled with various amines under the standard amide coupling conditions followed by removal of the *tert*-butyl or 4-methoxybenzyl group of the 2-aminoquinoline to give **51**−**57**.

The 6-substituted compounds in Table 6 were prepared from the intermediate **24** as shown in Scheme 8. Hydrolysis of the ester, then amide coupling with 3,3-dimethylbutanamine and hydrogenation of the olefin, provided **26**. Suzuki coupling of **26** with various boronic acids and removal of the *tert*-butyl or 4-methoxybenzyl group of the 2-aminoquinoline gave **60**−**62**. Alternatively, the bromide of **30** could be converted to the boronic ester **27** via palladium cross-coupling with bis-pinacol borane. Suzuki coupling of **27** with aryl halides, followed by removal of the 2-amino protecting group, afforded **58** and **59**.

RESULTS AND DISCUSSION

Fragment Screening and Subsequent SAR Development Using Protein X-ray Crystallography. The fragment library was designed to contain small, soluble, low-molecular-weight compounds that were selected by applying physicochemical filters, such as polar surface area (PSA) < 30 Å^2, the number of hydrogen bonding donors ≤2, and molecular weight <300. The library also included small heterocyclic compounds possessing functional groups which could form one or more polar or charged interactions with the two catalytic Asp residues in the BACE active site. Of particular interest were the known

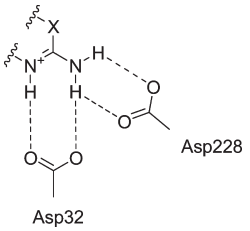

Figure 2. The binding mode of amidine-like groups with catalytic aspartates in the active site of BACE.

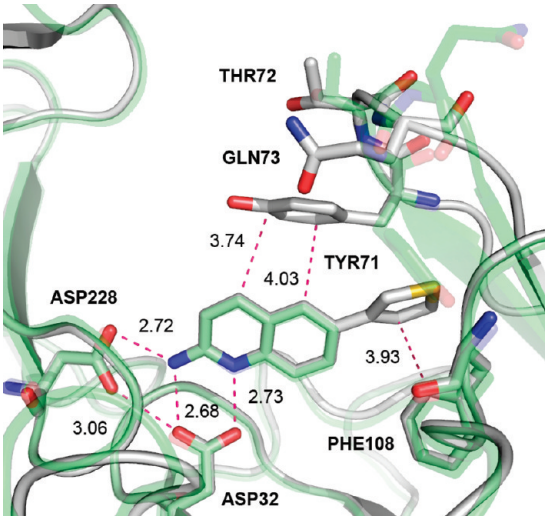

Figure 3. Co-crystal structure of **32** in BACE1 (white) superimposed with the 2-aminoquinoline co-crystal structure 2OHL (**1**, green.) Of note for **32** are the conformational change of flap Tyr71 and C−H···π interactions with Tyr71 and Phe108. Distances are reported in Å.

bidentate-type interactions afforded by aminoheterocycles and amidine-like moieties such as depicted in Figure 2.[30,31]

About 4000 compounds were chosen for screening. SPR technology was used to screen the fragment library rather than a fluorescence-based enzymatic assay because fluorescence-based detection is well-known to be susceptible to compound interference at high concentrations (>100 μM). SPR technology has been shown to be able to monitor and evaluate the relatively weak interactions with the target protein and allows for determination of binding constants >100 μM.[29c,32] After screening the fragment library, 106 fragment hits were identified with potency <10 mM by the SPR assay. These compounds were next tested in an ^{19}F-NMR-based functional assay which directly measured inhibition of BACE1 activity using a ^{19}F-labeled substrate peptide. Eight compounds were confirmed with potency less than 1 mM. These fragment hits (<1 mM) were further triaged based on LE, cocrystallization with the BACE1 protein, and initial SAR studies. Among these hits, 2-aminoquinoline **1** was characterized as a weak inhibitor with potency at 900 μM but excellent ligand efficiency at 0.38. These results are in the same range as reported previously by Astex,[30,31] who have also disclosed the binding modes for a number of aminoheterocyclic BACE1 inhibitors, including parent 2-aminoquinoline **1** with BACE1 (PDB accession code: 2OHL). In this structure, a C−H···π interaction (3.9−4.5 Å) is observed between the Tyr71 residue on the

Table 1. Activity of 2-Aminoquinoline and Bromo-Substituted 2-Aminoquinolines

Compound		SPR K_d (μM)	NMR K_i (μM)	Ligand Efficiency[a] kcal/N atom
1	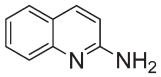	900	800	0.38
28	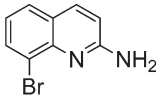	540	562	0.38
29	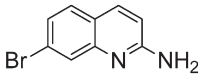	266	460	0.41
30	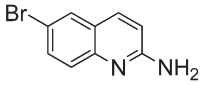	266	338	0.41
31	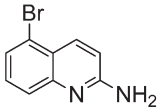	209	400	0.42

[a] Ligand efficiency is defined as free energy of binding per heavy atom and calculated based on K_d from SPR (LE = $\Delta G/N_{\text{non-hydrogen atoms}}$).

Table 2. Activity of 6-Substituted 2-Aminoquinolines

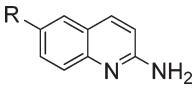

Compound	R	SPR K_d (μM)	Ligand Efficiency[a] kcal/N atom
32		38.8	0.38
33		22.6	0.37
34		10.6	0.38
35		10.8	0.38
36	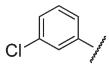	7.2	0.39
37	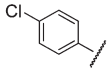	2000	-
38		296	0.28
39	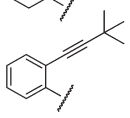	6.1	0.31

[a] Ligand efficiency is calculated based on K_d from SPR.

flap region of BACE1 and the 6-position of the 2-aminoquinoline core. This interaction is likely a significant driver of potency which complements the hydrogen bonding interactions between the basic N1 and the 2-amino group with aspartic acid residues 32 and 228, respectively (Figure 2). On the basis of the observed tight interaction between the carbon atom at the 6-position and the π face of Tyr71 in the binding of **1** with BACE, as well as its perpendicular trajectory with respect to the location of the BACE affinity pockets (e.g., P1, P1′, P2′), it would appear that substitution in the 6-position may not be well-tolerated as an access point to these various BACE subsites, which has been noted by others.[30] Nonetheless, we decided to examine the effect of adding a hydrophobic group at the various positions of the 2-aminoquinoline core using a bromine atom as shown in Table 1. Encouragingly, it was found that all of the bromo-substituted 2-aminoquinolines (**28**−**31**) displayed improved potency about 2−4 fold, with **29**, **30**, and **31** demonstrating higher ligand efficiency (0.41, 0.41, and 0.42 respectively) than parent 2-aminoquinoline **1**. Notably, the improved potency observed for **30** was striking in light of the existing cocrystal structure of **1**. We therefore decided to further investigated substitution at the 6-position with aryl groups (Table 2). Attachment of a thiophene (**32**) or phenyl (**33**) group at the 6-position resulted in a greater than 20-fold improvement in binding affinity. Compound **32** was cocrystallized with BACE enzyme and the superimposition of the cocrystal structures of **32** and the literature structure of **1** is shown in Figure 3[a].

Although both the protein backbone and the majority of the side chains in the region of the active site remain highly conserved, of note was the significant conformational change of Tyr71. This conformational change moves the Tyr71 side chain from the rear of the aminquinoline core to a position above it, resulting in C−H···π contacts between the face of the Tyr71 side chain and the 4- and 5- positions of the inhibitor. Moreover, the thiophene substituent at the 6-position engages in a C−H···π

dx.doi.org/10.1021/jm200544q | J. Med. Chem. 2011, 54, 5836–5857

Table 3. Activity of 3-Substituted and 3,6-Substituted 2-Aminoquinolines

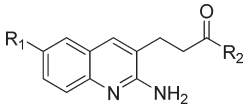

Compound	R_1	R_2	SPR K_d (μM)	BACE1 IC_{50} (μM)[a]	Ligand Efficiency kcal/N atom
40	H	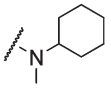	38.4	ND[b]	0.26[c]
41		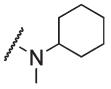	4.2	5.2	0.24[d]
42		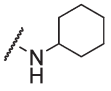	ND	0.074	0.34[d]
43		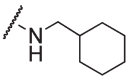	ND	0.034	0.30[c]
44	H	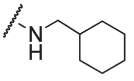	14.2	ND	0.30[c]

[a] IC_{50} values are the means of at least two experiments. [b] ND = not determined. [c] Ligand efficiency is calculated based on K_d from SPR. [d] Ligand efficiency is calculated based on IC_{50} from the FRET assay.

Table 4. α-Substituted Amide Aminoquinolines

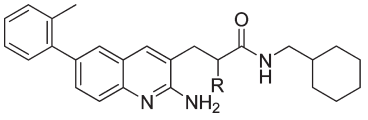

Compound	R	BACE1 IC_{50} (μM)[a]
45	*rac*-Me	0.0037
46	(*R*)-Me	0.0025
47	(*S*)-Me	0.97
48[b]		0.016
49[b]		0.027
50[b]		0.011

[a] IC_{50} values are the means of at least two experiments. [b] Racemic.

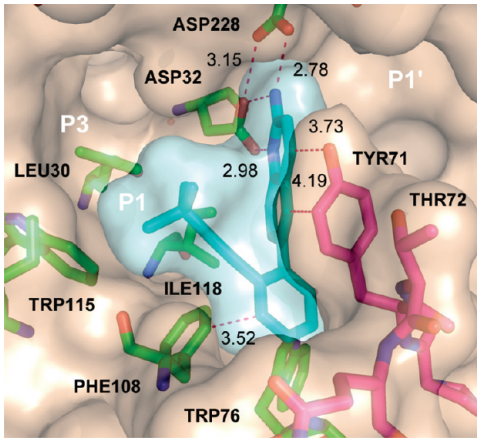

Figure 4. Co-crystal structure of **39** (light-blue with surface shown) in BACE1 (green with beige surface; flap residues shown in magenta) depicting occupancy of the P1 subsite by the *tert*-butyl alkyne of **39**. Distances are reported in Å.

interaction with the edge of Phe108. The overall binding motif is reminiscent of that of a dihydroquinazoline class of BACE1 inhibitors previously reported in the literature.[30]

Substitution at both *ortho* (**34** and **35**) and *meta* (**36**) position of the C-6 aryl ring enhanced the potency by about 2-fold while retaining good ligand efficiency, whereas *para* substitution of the phenyl ring (**37**) was not tolerated. Compound **38**, with a cyclohexyl group at the 6-position showed a 13-fold loss in potency, underlining the importance of the edge−face interaction between Phe108 and the face of the 6-aryl group as a significant source of binding affinity.

The *ortho* position of the 6-phenyl group appeared to furnish an access point into the P1 affinity pocket. Analogues such as the *tert*-butyl alkyne derivative **39** were synthesized to explore this area, with the predicted binding in the P1 verified by crystallography (Figure 4). Although **39** displayed a 3.7-fold increase in

dx.doi.org/10.1021/jm200544q | *J. Med. Chem.* 2011, 54, 5836–5857

Table 5. 3-Substituted Amide 2-Aminoquinolines

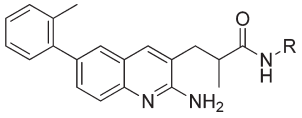

Compound	R	IC_{50} (μM)[a]		Cell Shift	Papp	ER[e]	cLogP[f]
		BACE1	Cell	Cell IC_{50}/FRET IC_{50}	(nm/s)		
51[c]	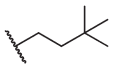	0.00065	0.25	380	65	0.9	5.6
52[c]	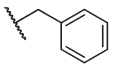	0.020	5.1	260	65	0.8	5.5
53[b]	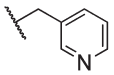	0.088	0.56	6.4	160	8.2	3.5
54[b]	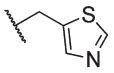	0.031	0.43	14	120	6.7	3.3
55[c]	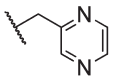	0.050	0.49	10	200	29.4	2.5
56[c]	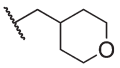	0.010	0.17	17	120	24.7	3.2
57[c,d]	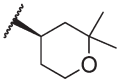	0.0007	0.018	26	89	5.8	3.6

[a] IC_{50} values are the means of at least two experiments. [b] Racemic. [c] (*R*)-isomer. [d] (*R*)-isomer at the pyran ring determined by X-ray crystal structure. [e] Efflux ratio in LLC-PK cells transfected with rat MDR1. [f] cLogP values are calculated by Daylight Toolkit 4.81.

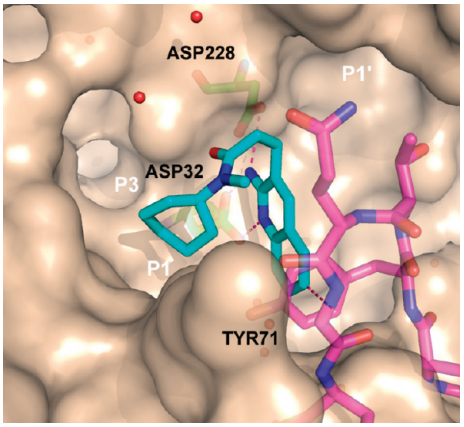

Figure 5. Co-crystal structure of **40** (light-blue) in BACE1 (green with beige surface; flap residues in transparent magenta) depicting occupancy of the P1 subsite by the *N*-cyclohexyl substituent.

potency compared to the 6-phenyl substituted parent compound **33**, and modest 2-fold improvement over the much smaller methyl and chloro-substituted analogues **34** and **35**, it rendered an overall decrease in LE compared to the latter two analogues. This decrease in LE occurred despite the introduction of the highly shape-complementary *tert*-butyl hydrophobic group in the roughly spherical P1 affinity pocket along with the utilization of a spacer of seemingly ideal length and possessing a minimal number of rotatable bonds.

The P1 pocket is comprised in part by aromatic residues Phe108 and Trp115, and thus aromatic rather than purely aliphatic hydrophobic substitution in P1 might be expected to furnish some additional potency. However, it was projected that such potency gains in P1 might not be commensurate with the molecular weight and hydrophobicity expense necessary to access it. We therefore sought to identify other opportunities to access the various affinity pockets of BACE1 from other positions on the 2-aminoquinoline core, which might increase binding affinity in a more ligand efficient manner.

Akin to a previously reported class of dihydroquinazoline inhibitors[18] found to access the P1 affinity site, amide substitution at the 3-position of the aminoquinoline core was pursued. Compound **40** was prepared and cocrystallized with the BACE1 enzyme (Table 3). The crystal structure demonstrated that the side chain conformation at the 3-position was similar to that observed in the literature, with preferential occupation of the P1 pocket by the cyclohexyl substituent of the *N*,*N*-disubstituted amide (Figure 5). In the absence of a 6-substituent, the conformation of overhead Tyr71 in the structure of **40** reverted to that observed in the structure of the parent aminoquinoline, re-engaging the 5- and 6-positions in a C−H···π interaction (cf. 4- and 5-position in **7**, Figure 3).

The potency of **40** via SPR measurement was 38.4 μM, 23-fold more potent than parent 2-aminoquinoline **1**. Addition of the

dx.doi.org/10.1021/jm200544q | *J. Med. Chem.* 2011, 54, 5836–5857

Table 6. C-6 Substituted 3,3-Dimethylbutyl Amide 2-Aminoquinolines

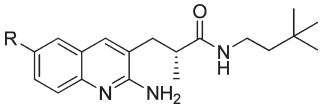

Compound	R	IC_{50} (μM)[a] BACE1	IC_{50} (μM)[a] Cell	Cell Shift Cell IC_{50}/FRET IC_{50}	Papp (nm/s)	ER[d]	clogP[e]
58[c]		0.016	0.035	2.2	150	7.8	4.2
59[c]		0.011	0.080	8.0	120	3.1	4.4
60[b]	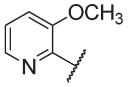	0.097	0.25	2.6	130	9.0	3.8
61[b]	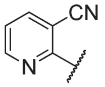	0.39	1.7	4.4	150	4.1	3.3
62[b]	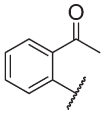	0.015	0.11	7.3	120	1.8	4.6

[a] IC_{50} values are the means of at least two experiments. [b] Racemic. [c] (*R*)-isomer. [d] Efflux ratio in LLC-PK cells transfected with rat MDR1. [e] cLogP values are calculated by Daylight Toolkit 4.81.

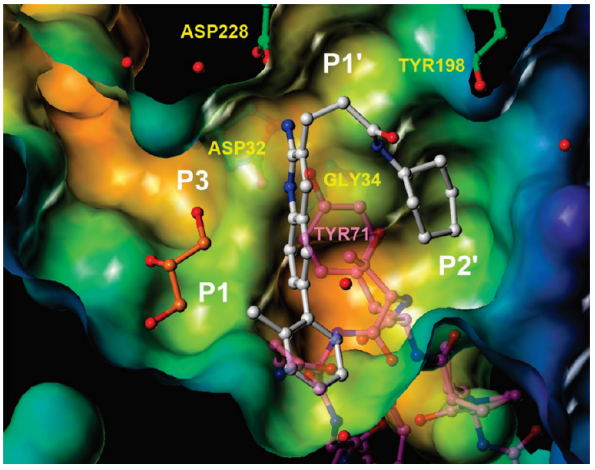

Figure 6. Co-crystal structure of **42** (white) in BACE1 (cutaway surface view), depicting P2′ subsite binding of the *N*-cyclohexyl moiety. Flap residues (surface not shown) in transparent magenta, active site residues in green, and BACE1 active site surface colored by cavity depth. Occupation of P1 by a glycerol molecule (from cryoprotectant in crystallography sample) is depicted in orange.

optimal 6-tolyl group gave rise to **41** (ca. 4 μM), 9-fold more potent than **40** and 2-fold improved over **34**. At this point, the observed potencies were entering a range (<10 μM) where it was possible to accurately compare and verify SPR measurements via our standard enzymatic assay, which were found to be consistent for **41** (4.2 and 5.2 μM, respectively).

Although the potency of **40** and **41** were improved versus their respective parent compounds which lacked the 3-side chain (**1** and **34**), their LE were significantly less than that of both **34** and parent 2-aminoquinoline **1** (0.26 vs 0.38 and 0.24 vs 0.38, respectively). This suggested that occupancy of P1 pocket via a tethered, *N*,*N*-disubstituted amide side chain might not lead to high-efficiency binding to the BACE1 protein. The observed gains in potency were, in our view, insufficient to offset the increase in molecular weight necessary for P1 occupancy.

However, removal of the *N*-methyl group on the pendant amide function, coupled with an *o*-tolyl substituent at the 6-position (**42**), resulted in an astonishing increase in potency, with an IC_{50} value of 0.074 μM. This represented a 123-fold improvement over **34** and approaching 10500-fold over the initial fragment hit **1**. The cocrystal structure of **42** with the BACE enzyme revealed that the 3-amide chain was no longer oriented toward the P1 side of the active site. Instead, the *N*-cyclohexyl occupies the P2′ region, with the NH of the pendant amide forming a hydrogen bonding interaction with the carbonyl oxygen of Gly34 on the underside of the active site (Figure 6). This contact is augmented by an interaction between the amide π face and the edge of nearby Tyr198. The *o*-methyl group of the 6-tolyl function is oriented toward the P1 site. In addition, the structure also revealed the P2′ site was not fully occupied by the cyclohexyl amide group, indicating that an amide group with longer alkyl chain might extend further into the P2′ pocket, allowing for higher binding affinity. In light of this observation, we added a simple methylene linker and prepared cyclohexylmethyl amide analogue **43**. Indeed, **43** exhibited an IC_{50} value of 34 nM in the enzymatic assay, a 2-fold improvement over **42**.

The presence of the 6-tolyl substitution appears to direct the 3-amide group away from the nonprime region and into the P1′/P2′ affinity sites, likely due in part to the presence of the *o*-methyl

dx.doi.org/10.1021/jm200544q | *J. Med. Chem.* 2011, 54, 5836–5857

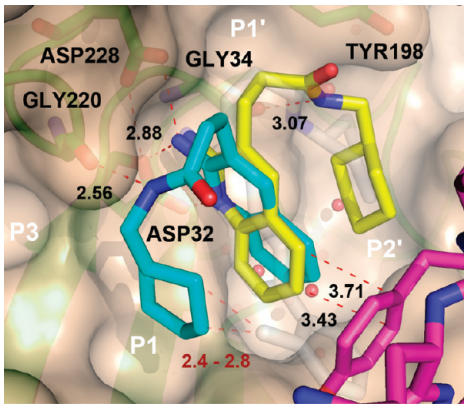

Figure 7. Co-crystal structure of **44** (cyan and yellow) in BACE1 (cutaway surface in beige; active site residues in green, flap residues in magenta) depicting dual binding conformations occupying both the P1 and P2′ affinity pockets. Superimposed (based on crystal structure alignment) is **42** from Figure 6 (transparent white). Distances are reported in Å.

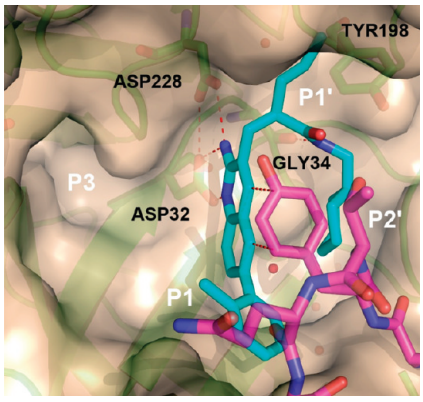

Figure 8. Co-crystal structure of **50** (cyan) in BACE1 (cutaway surface in beige; active site residues in green, flap residues in magenta) depicting occupancy of P1′ and P2′.

group oriented toward P1. Interestingly, compound **44**, the direct *des*-tolyl analogue of **43**, cocrystallizes in BACE1 in both prime- and nonprime-site binding conformations, as seen clearly from the electron density (Figure 7). In each of the two, nearly *Cs*-symmetric binding conformations, the amide NH from the inhibitor engages the C═O of a glycine residue on the underside of the active site (Gly34 and Gly230), orienting the cyclohexylmethyl substituent into both the P1 and P2′ subsites. For 6-tolyl analogue **43**, nonprime-site binding of this hydrophobic group would likely not be possible due to an intramolecular steric clash (ca. 2.4−2.8 Å) illustrated by the alignment of the crystallographic poses of **44** and **42** (Figure 7).

With two hydrogen bond donors and molecular weight below 400, the lead compound **42** displayed good BACE1 potency with high LE at 0.34. This compound was evaluated in the cell-based Aβ production assay (Aβ40) and showed moderate activity with an IC_{50} = 0.71 μM. Additionally, we employed an in vitro permeability assay using LLC-PK cell line transfected with human or rat Pgp to estimate passive blood−brain barrier permeability and efflux susceptibility.[34] For CNS penetrable compounds, the targeted in vitro passive permeability is >100 nm/s with an efflux ratio (ER) less than 3.[9a,35] The LLC-PK assay showed that **42** had modest permeability (66 nm/s) and low ER at 0.6. Overall, the results indicated that compound **42** represented a promising profile as a lead compound for further development into CNS penetrable BACE1 inhibitors. We therefore carried out SAR studies on this compound, particularly focused on improving cell potency and permeability.

Optimization of 2-Aminoquinoline Lead Compound 42: Conformational Stabilization and P1′ Access. Analysis of the binding of **42** with BACE1 protein revealed that an α-alkyl substituent in the (*R*)-configuration (*anti* with respect to the quinoline core) should enhance binding affinity via enrichment of the binding (amide-*gauche*) conformation by destabilization of other rotamers about the $C_{benzyl}-C_{\alpha}$ σ bond. Such a substituent would also be ideally poised to occupy the previously empty P1′ pocket (Figure 6). To investigate this strategy, a series of α-substituted amide analogues of **43** were prepared (Table 4). A simple α-methyl group (**45**) showed single-digit nanomolar potency at 3.7 nM, which is nearly a 10-fold increase over *des*-methyl analogue **43**. The (*R*)-isomer **46** was preferred to the (*S*)-isomer **47** (2.5 nM vs 970 nM in the FRET assay). Larger α-amide groups **48**, **49**, and **50** (all racemic), however, afforded less potent analogues versus α-methyl analogue **45** (racemic), suggesting that the (*R*)-isomer of α-methyl substituent was optimal. Successful cocrystallization of α-propyl analogue **50** as its racemic mixture confirmed the occupation of the P1′ and P2′ subsites by the (*R*)-enantiomer (Figure 8).

Having secured the optimal α-amide substitution, attention shifted to exploring the P2′ region. This region of the molecule appeared to be fairly accommodating, accepting alkyl groups as well as saturated and unsaturated ring systems. The results for the amide analogues are provided in Table 5. Compound **51** was designed to have a longer alkyl chain, and the 3,3-dimethylbutanyl group can position deeper into the P2′ pocket. This compound achieved subnanomolar BACE1 potency at 0.65 nM in the enzymatic assay. The benzyl group of **52** was also tolerated and showed potency at 20 nM in the enzymatic assay. However, both compound **51** and **52** showed large cell shifts (380-fold and 260-fold, respectively) and modest permeability (65 and 65 nm/s, respectively), most likely due to the high cLogP (5.6 and 5.5, respectively) of these two compounds. In an attempt to improve permeability and reduce cell shift, polarity was introduced through heteroaryl derivatives such as pyridin-3-ylmethanamide **53**, thiazol-5-ylmethanamide **54**, and pyrazin-2-ylmethanamide **55**, each having lower cLogP at 3.5, 3.3, and 2.5, respectively. Although these heteroaryl analogues showed comparable or slightly decreased enzyme activity (**53** and **54** are racemic) as compared to the benzylamide **52**, the above-mentioned analogues demonstrated much improved cell shift versus **52** (6.4−14-fold vs 260-fold) as well as improved permeability (160, 120, and 200 nm/s respectively). Unfortunately, these heteroaryl compounds all showed elevated ER in both rat and human transfected Pgp cell lines (ER data in rat shown in Table 5). We also introduced a heteroatom to saturated ring systems (**56** and **57**). **56** containing a tetrahydropyran group that had cLogP of 3.2, displayed good potency in the enzymatic assay at 10 nM and cell potency of 0.17 μM with relatively low cell shift (17-fold). This compound also had good permeability (120 nm/s), but the ER was high at 25. To modulate the polarity and reduce Pgp-mediated efflux, a *gem*-dimethyl group was introduced next to the oxygen atom on the pyran ring in **57**. This compound possessed cLogP of 3.6 and demonstrated excellent

dx.doi.org/10.1021/jm200544q | *J. Med. Chem.* 2011, 54, 5836–5857

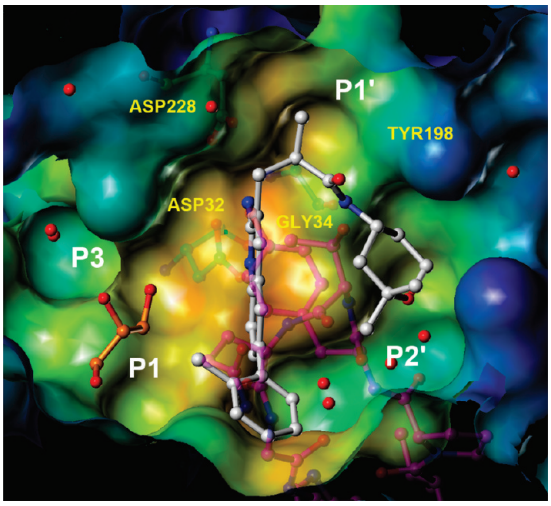

Figure 9. Co-crystal structure of **57** (white) in BACE1 (cutaway surface view), depicting P1′ and P2′ subsite binding of the α-methyl and *N*-dimethylpyranyl groups, respectively. Flap residues (surface not shown) in transparent magenta, active site residues in green, and BACE1 active site surface colored by cavity depth. Occupation of P1 by a glycerol molecule (from cryoprotectant in crystallography sample) is depicted in orange.

potency in the enzymatic assay at 0.7 nM and good cell potency at 18 nM. The permeability was moderate at 89 nm/s, and the ER was notably decreased compared to **56** (5.8 vs 25). These results and subsequent investigation on the relationship of cLogP with permeability and cell shift of aminoquinoline compounds suggested that it is essential to design compounds with cLogP values below 5 in order to achieve good permeability as well as low cell shift. Compound **57** was crystallized in BACE1 (Figure 9) as its single (*R*) enantiomer at the P1′ occupying, α-methyl position. The single configuration at the pyran substituent, while not confirmed via synthesis, was determined from the electron density to be (*R*).

In the effort to optimize the physical properties, a number of polar substitution groups at 6-position were also investigated. The 3,3-dimethylbutanyl amide group that offered the best potency was used at the P2′ region. The SAR of 6-substitutions revealed that the pyridin-2-yl group is tolerated (**58**−**61**, Table 6). The cell shift was only 2-fold with the 3-methyl pyridine-2-yl analogue **58**, having an IC_{50} of 16 nM in the enzymatic assay and 35 nM in the cell assay. This compound also had good permeability at 150 nm/s, however, the ER was 7.8. The 3-chloro pyridin-2-yl analogue **59** exhibited potency of 11 nM in the enzymatic assay and 80 nM in the cell assay. The permeability was 120 nm/s with a desirable ER of 3.1. The 3-methoxy and 3-cyano pyridine-2-yl analogues **60** and **61** showed less potency in the enzymatic and the cell assay, but both of these compounds had good permeability (130 and 150 nm/s, respectively). The *o*-methylketone phenyl analogue **62** also showed good potency in the enzymatic assay (15 nM) as well as in the cell assay (110 nM), demonstrating good permeability (120 nm/s) and low ER at 1.8. The cLogP is lower than 5 for all of these compounds (**58**−**62**) that exhibited low cell shift (<10) and good permeability (>100 nm/s). This result indicated that we could improve cell potency as well as achieve good permeability by modification of the physical properties.

To elucidate the value of these aminoquinolines in reducing Aβ in vivo, we chose **59** for further investigation in a rat model.

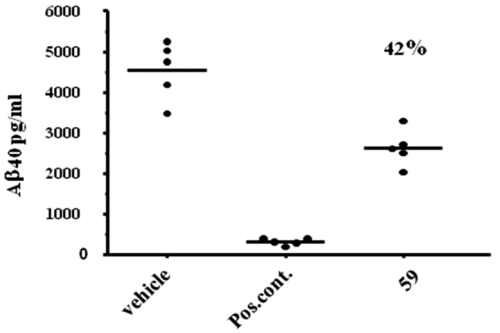

Figure 10. Aβ40 reduction of **59** in CSF observed in the rat PD model. A known γ-secretase inhibitor, (*S*)-2,3-dimethyl-*N*-((*S*)-1-(((*S*)-5-methyl-6-oxo-6,7-dihydro-5*H*-dibenzo[*b*,*d*]azepin-7-yl)amino)-1-oxopropan-2-yl)butanamide, was used as a positive control.[36]

Compound **59** had desired overall properties in cell potency, permeability, and ER. Dosed at 60 mg/kg subcutaneously, compound **59** was evaluated in the rat PD model for lowering of Aβ40/42 measured in the CSF. Evaluated at the 2 h time point, **59** showed a significant 42% reduction of CSF Aβ40/42 formation after a single dose ($p < 0.0001$) (Figure 10). This result demonstrated that with desired properties, the 2-aminoquinoline BACE1 inhibitor **59** was able to afford good CNS penetration and produce significant in vivo efficacy in Aβ reduction. Unfortunately, compound **59** displayed high human and rat microsomal clearance. Efforts to improve metabolic stability of this class of compounds will be the focus of future efforts.

CONCLUSION

Using SPR to screen a focused fragment library, 2-aminoquinoline **1** was identified as an initial fragment hit that displayed potency in the millimolar range. A rapid optimization of the 2-aminoquinoline hit guided by LE and supported by X-ray crystal structures led to the identification of a lead compound **42** with a potency of 74 nM for BACE1, reflecting a 12000-fold increase in potency over the starting fragment hit while preserving ligand efficiency. Further SAR investigation delivered potent BACE inhibitors in the subnanomolar range with over 10^6-fold increase in potency. Subsequently, modification of the physical properties of these 2-aminoquinoline analogues led to further improvements including decreasing the enzyme/cell shift, improving permeability, and lowering ER, culminating in potent BACE1 inhibitors with desirable properties for CNS penetration. Compound **59** exemplified these improvements displaying significant Aβ reduction in CSF in a rat PD model.

EXPERIMENTAL SECTION

SPR Assay. Dissociation constant (K_d) measurements were performed on Biacore S51 and T100 instruments (GE Healthcare). BACE1 protein and inhibitors for Biacore measurements were generated in-house; all other reagents were purchased from GE Healthcare or Sigma-Aldrich. Glycosylated BACE1 was reacted with sodium periodate to oxidize *cis*-diols groups on sugar chains to aldehydes. The oxidized BACE was immobilized at high density (10000−12000 RU) onto CM5 chips using aldehyde coupling chemistry and resulted in surface activities close to 100% based on binding of a reference inhibitor, *N*-((2*S*,3*S*,5*R*)-6-((1*S*,2*S*,4*R*)-bicyclo[2.2.1]heptan-2-ylamino)-3-hydroxy-5-methyl-6-oxo-1-phenylhexan-2-yl)-3-(2-oxopyrrolidin-1-yl)benzamide. The immobilization running buffer consisted of 10 mM HEPES pH 7.4 with

150 mM NaCl, and immobilization steps consisted of a 3−4 min EDC/NHS activation step [200 mM 1-ethyl-3-(3-dimethylaminopropyl) carbodiimide hydrochloride, 50 mM *N*-hydroxysuccinimide], 7 min 5 mM carbohydrizide in water, 7 min 1 M ethanolamine hydrochloride pH 8.5, 10 min 20 μg/mL oxidized BACE in 10 mM sodium acetate pH 4.0, 7 min 100 mM sodium cyanoborohydride in 100 mM sodium acetate pH 4.0, 3 × 30 s 50 mM glycine pH 9.5, and 3 × 30s 1 M NaCl in 100 mM $NaHCO_3$ pH 9.5.

For K_d measurements the buffer was replaced with 50 mM sodium acetate pH 5.0, 150 mM NaCl, 0.005 (v/v) Tween20, and 5% (v/v) DMSO. Compound stocks prepared in DMSO (typically 20 mM) were serially diluted in running buffer and injected over the immobilized BACE1. Association and dissociation time were typically set to 45 s and 90 s, respectively. The runs were performed at 25 °C with a flow rate from 10 to 90 μL/min and data collection rate of 10 Hz.

The data was processed and analyzed using Scrubber-2 analysis software (BioLogic Software, Campbell, Australia). The sample response observed on the reference spot was subtracted from the sample response with immobilized BACE1 to correct for systematic noise and baseline drift. Data was solvent corrected and the response from blank injections was used to double-reference the binding data. The data was molecular weight normalized and K_d values established using simple steady analysis with one global R_{max} (or individual R_{max} in cases were complete saturation was achieved).

BACE1 ^{19}F NMR Enzymatic Assay. An NMR-based enzymatic assay was designed using a ^{19}F-labeled BACE1 substrate peptide with the sequence EVNLDAEF(CF_3). BACE1 cleaves this peptide between the L and D residues, which resulted in distinct ^{19}F NMR signals for the substrate and product. Integration of the signal area yielded concentrations of each component and allowed calculation of K_i. The assay was conducted in 96-well plate format using 200 nM of BACE1 reacted with 100 μM of the substrate peptide. Compounds of interest were added at various concentrations and were followed with a blank DMSO control well as well as a control inhibitor with a K_i of 400 nM. The experiment was conducted in 25 mM sodium acetate, pH 5.0, and allowed to react for a period of 20 min, at which time the reaction was quenched by the addition of 300 μL of 8 M urea (20% D_2O for NMR frequency lock). All experiments were conducted on a Bruker Avance III 500 MHz NMR spectrometer with an SEF cryoprobe for ^{19}F direct detection.

BACE1 Enzymatic Assay. BACE1 enzymatic activity was determined by the enhancement of fluorescence intensity upon enzymatic cleavage of the fluorescence resonance energy transfer substrate. The BACE recognition and cleavage sequence of the substrate is derived from the reported literature,[37] and the fluorophore and quencher dyes are attached to side chain of Lys residues at the termini of the substrate peptide. The human recombinant BACE1[38] assay was performed in 50 mM acetate, pH 4.5/8% DMSO/100 μM Genepol/0.002% Brij-35. In dose−response IC_{50} assays, 10 point 1:3 serial dilutions of compound in DMSO were preincubated with the enzyme for 60 min at room temperature. Subsequently, the substrate was added to initiate the reaction. After 60 min at room temperature, the reaction was stopped by addition of 0.1 M Tris base to raise the pH above the enzyme active range, and the increase of fluorescence intensity was measured on Safire II microplate reader (Tecan, Männedorf, Switzerland).

Cell-Based Assay. Human embryonic kidney cells (HEK293) stably expressing APP_{SW} were plated at a density of 100K cells/well in 96-well plates (Costar). The cells were cultivated for 6 h at 37 °C and 5% CO_2 in DMEM supplemented with 10% FBS. Cells were incubated overnight with test compounds at concentrations ranging from 0.0005 to 10 μM. Following incubation with the test compounds the conditioned media was collected and the Aβ40 levels were determined using a sandwich ELISA. The IC_{50} was calculated from the percent of control Aβ40 as a function of the concentration of the test compound. The sandwich ELISA to detect Aβ40 was performed in 96-well microtiter plates, which were precoated with goat antirabbit IgG (Pierce). The capture and detection antibody pair that was used to detect Aβ40 from cell supernatants consists of affinity purified pAβ40 (Invitrogen) and biotinylated 6E10 (Covance), respectively. Conditioned media was incubated with capture antibody overnight at 4 °C, followed by washing. The detecting antibody incubation was for 3 h at 4 °C, again followed by the wash steps as described previously. The plate was developed using Delfia reagents (Streptavidin-Europium and Enhancement solution (Perkin-Elmer)) and time-resolved fluorescence was measured on an EnVision multilabel plate reader (Perkin-Elmer).

Permeability Assay. The wild-type cell line LLC-PK1 (porcine renal epithelial cells, WT-LLC-PK1) was purchased from American Type Culture Collection (ATCC, Manassass, VA). Transfections of WT-LLC-PK1 cells with human *MDR1* gene (hMDR1-LLC-PK1) and rat *mdr1a* gene (rMdr1a-LLC-PK1) were generated. Cells were grown in Medium 199 supplemented with 10% fetal bovine serum.[39] Cells were seeded onto matrigel-coated transwell filter membranes at a density of 90000 cells/well. Media change was performed on day 3. Compound incubations were performed 5−6 days post seeding. All cultures were incubated at 37 °C in a humidified (95% relative humidity) atmosphere of 5% CO_2/95% air.

Prior to the transport experiment,[40] culture medium was aspirated from both apical and basolateral wells, and cells were rinsed with warmed (37 °C) Hank's balanced salt solution supplemented with 10 mM Hepes at pH 7.4 (HHBSS, Invitrogen, Grand Island, NY). HHBSS was removed from wells prior to dosing with test drugs at 5 μM in transport buffer (HHBSS containing 0.1% bovine serum albumin). Then 150 μL of transport buffer were added to receiver chambers prior to dosing in triplicate to apical or basolateral chambers. The dosed transwell plates containing the cell monolayers were incubated for 2 h at 37 °C on a shaking platform. At the end of the incubation period, 100 μL samples were collected from receiver reservoirs and analyzed by LC-MS/MS on an API4000 (Applied Biosystem, Foster City, CA) triple quadruple mass spectrometer interfaced with turbo IonSpray operated in positive mode using Analyst 1.4.2 software.

The apparent permeability coefficient (P_{app}) of all tested agents was estimated from the slope of a plot of cumulative amount of the agent versus time based on the following equation:

$$P_{app} = (dQ/dt)/(A \cdot C_0)$$

where dQ/dt is the penetration rate of the agent (ng/s), A is the surface area of the cell layer on the Transwell (0.11 cm^2), and C_0 is the initial concentration of the test compound (ng/mL). Efflux ratio (ER) was calculated from the basolateral-to-apical permeability divided by the apical-to-basolateral permeability: ER = P_{app} $B > A/P_{app}$ $A > B$.

X-ray Crystal Structure. Recombinant human BACE1 residues 14−453 was overexpressed in bacteria as inclusion bodies and refolded using a procedure described by Patel et al.[41] Crystals were grown in similar conditions described in Patel et al.[41] BACE1 protein was concentrated to 8 mg/mL in a buffer containing 20 mM Tris (pH 8.2), 150 mM NaCl, and 1 mM DTT. DMSO (3% v/v) was added to the protein immediately prior to crystallization. Apo crystals of BACE1 were grown at 20 °C using the hanging drop method/vapor diffusion method, the drops containing 1 μL of BACE1 solution and 1 μL of reservoir solution. The reservoir solution consisted of 20% (w/v) PEG 5000 monomethylethyl ether (MME), 200 mM sodium citrate (pH 6.6), and 200 mM sodium iodide. Apo BACE1 crystal was soaked overnight in a 5.0 mM compound solution with 33% (w/v) PEG 5000 monomethylethyl ether (MME), 110 mM sodium citrate, 220 mM sodium iodide, and 10% DMSO (from compound dilution). The following day, the crystal was briefly transferred to a cryoprotectant (5.0 mM compound with 33% (w/v) PEG 5000 monomethylethyl ether (MME), 110 mM sodium citrate, 220 mM sodium iodide, 10% DMSO and 22% glycerol)

and flash frozen in liquid nitrogen. Data was collected at Advanced Light Source Beamline 5.0.2 (Lawrence Berkeley National Laboratory, Berkeley, CA) at 100 K. Data was processed and scaled using HKL2000.[42] The crystals belong to the space group $P6_122$ with approximate unit cell dimensions of $a = b = 103$ Å, $c = 169$ Å. Molecular replacement was performed using Phaser,[43] using an apo BACE-1 structure (PDB entry 1w50) as a search model. The structure was refined using Refmac 5,[44] and the model with ligand was built with Coot.[45]

Pharmacodynamic Assay. Male Sprague−Dawley rats (175−200 g) were purchased from Harlan and were maintained on a 12 h light/dark cycle with unrestricted access to food and water until use. Rats were dosed subcutaneously with **59** at 20 and 60 mg/kg in 15% HPBCD, pH 4. Rats were euthanized with CO_2 inhalation for 2 min, and cisterna magna was quickly exposed by removing the skin and muscle above it. CSF (50−100 μL) was collected with a 30 gauge needle through the dura membrane covering the cisterna magna. Blood was withdrawn by cardiac puncture and plasma obtained by centrifugation for drug exposures. Brains were removed and, along with the CSF, immediately frozen on dry ice and stored at −80 °C until use. The frozen brains were subsequently homogenized in 10 volumes of (w/v) of 0.5% Triton X-100 in TBS with protease inhibitors. The homogenates were centrifuged at 100000 rpm for 30 min at 4 °C. The supernatants were analyzed for Aβ40 levels by immunoassay as follows: Meso Scale 96-well avidin plates were coated with Biotin-4G8 (Covance) and detected with ruthenium-labeled Fab specific for Aβ40. Plates were read in MSD Sector6000 imager according to manufacturer's recommended protocol (Meso Scale Discovery, Inc.). Aβ40 concentrations were plotted using Graphpad Prism and analyzed by one-way ANOVA followed by Dunnett's multiple comparison analysis to compare drug-treated animals to vehicle-treated controls.

Chemistry. Unless otherwise noted, all materials were obtained from commercial suppliers and used without further purification. Anhydrous solvents were obtained from Aldrich or EM Science and used directly. All reactions involving air- or moisture-sensitive reagents were performed under a nitrogen or argon atmosphere. All microwave assisted reactions were conducted with a Smith synthesizer from Personal Chemistry, Uppsala, Sweden. Silica gel chromatography was performed using either glass columns packed with silica gel (230−400 mesh, EMD Chemicals, Gibbstown, NJ) or prepacked silica gel cartridges (Biotage or ISCO). ^{1}H NMR spectra were determined with a Bruker 300 MHz or DRX 400 MHz spectrometer. Chemical shifts are reported in parts per million (ppm, δ units) downfield from tetramethylsilane. All tested compounds were purified to ≥95% purity as determined by reverse phase HPLC. HPLC analysis was obtained on Agilent 1100, using one or two of the following three methods. HPLC method A (3.6 min LC-MS run): Zorbax analytical C18 column (50 mm × 3 mm, 3.5 μm, 40 °C); mobile phase, A = 0.1% TFA in water, B = 0.1% TFA in acetonitrile; gradient, 0.0−3.6 min, 5−95% B; flow rate = 1.5 mL/min; 254 nm; 0 min post time; 1.0 μL injection. HPLC method B (10 min LC-MS run): YMC ODS-AM (100 mm × 2.1 mm, 5 μm, 40 °C); mobile phase, A = 0.1% HCOOH in water, B = 0.1% HCOOH in acetonitrile; gradient, 0.0−0.5 min, 10% B; 0.5−7.0, 10−100% B; 7.0−10 min, 100% B; flow rate = 0.5 mL/min; 254 nm; 1.5 min post time; 3.0 μL injection. HPLC method C (5 min LC-MS Run): Phenomenex Synergi MAX-RP (50 mm × 2.0 mm, 4.0 mm, 40 °C); mobile phase, A = 0.1%TFA in water, B = 0.1% TFA in acetonitrile; gradient, 0.0−0.2 min, 10% B, 0.2−3.0 min, 10−100% B, 3.0−4.5 min 100% B, 4.5−5.0 min, 100−10% B; flow rate = 0.8 mL/min; 254 nm; 1.5 min post time; 3.0 μL injection. Low-resolution mass spectral (MS) data were determined on a Perkin-Elmer-SCIEX API 165 mass spectrometer using ES ionization modes (positive or negative).

8-Bromoquinolin-2-amine (28). 8-Bromoquinolin-2-ol (3.16 g, 14 mmol) was mixed with phosphorus oxychloride (40 mL, 429 mmol) and heated to reflux in a 140 °C oil bath for 2 h. The mixture was allowed to cool to room temperature and then evaporated to dryness under reduced pressure. Then ice water was added to the resulting residue followed by dichloromethane (80 mL). This mixture was stirred, and potassium carbonate was added carefully until the mixture had been neutralized to pH 7. The organic phase was separated and dried with magnesium sulfate, filtered, and concentrated to dryness under reduced pressure. This crude material was dissolved in a mixture of dry ethanol (12 mL) and toluene (4 mL) with heating and was transferred to a microwave vessel. 4-Methoxybenzylamine (1.6 mL, 12 mmol) was added, and the vial was sealed and heated to 155 °C for 45 min. Then the reaction was evaporated to dryness under reduced pressure and purified by column chromatography on silica gel (eluting with a gradient of 20−100% ethyl acetate in hexane) to give *N*-(4-methoxybenzyl)-8-bromoquinolin-2-amine. This material was dissolved in trifluoroacetic acid (20 mL) and heated to 60 °C for 90 min and then evaporated to dryness under reduced pressure. The residue was purified by column chromatography on silica gel (eluding with a gradient of 50−100% ethyl acetate in hexane) to give the 8-bromoquinolin-2-amine (0.102 g, 3.2% yield over 3 steps) as a brown solid. ^{1}H NMR (400 MHz, methanol-d_4) δ 8.37 (d, J = 9.4 Hz, 1H), 8.09 (dd, J = 7.8, 1.2 Hz, 1H), 7.93 (dd, J = 7.9, 1.1 Hz, 1H), 7.46 (t, J = 7.9 Hz, 1H), 7.16 (d, J = 9.4 Hz, 1H), 4.8 (br s, 2H). MS (ESI, positive ion) m/z: 223 (M + 1).

7-Bromoquinolin-2-amine (29). Using 2-aminoquinolin-7-ol and following the procedure used to prepare **28** gave **29**. ^{1}H NMR (400 MHz, chloroform-*d*) δ 7.81−7.88 (m, 2H), 7.47 (d, J = 8.4 Hz, 1H), 7.35 (dd, J = 8.5, 1.9 Hz, 1H), 6.72 (d, J = 8.8 Hz, 1H, 5.27 (br s, 2H). MS (ESI, positive ion) m/z: 223 (M + 1).

6-Bromoquinolin-2-amine (30). Using 2-aminoquinolin-6-ol and following the procedure used to prepare **28** gave **30**. ^{1}H NMR (400 MHz, chloroform-*d*) δ 7.72−7.78 (m, 2H), 7.60 (dd, J = 8.8, 2.5 Hz, 1H), 7.52 (d, J = 8.8 Hz, 1H), 6.73 (d, J = 8.8 Hz, 1H), 5.1 (br s, 2H). MS (ESI, positive ion) m/z: 223 (M + 1).

5-Bromoquinolin-2-amine (31). Using 2-aminoquinolin-5-ol and following the procedure used to prepare **28** gave **31**. ^{1}H NMR (400 MHz, chloroform-*d*) δ 8.28 (d, J = 9.0 Hz, 1H), 7.63 (d, J = 8.1 Hz, 1H), 7.53 (d, J = 8.0 Hz, 1H), 7.40 (t, J = 8.0 Hz, 1H), 6.80 (d, J = 9.0 Hz, 1H), 5.14 (br s, 2H). MS (ESI, positive ion) m/z: 223 (M + 1).

6-(Thiophen-3-yl)quinolin-2-amine (32). A mixture of thiophen-3-ylboronic acid (0.25 mmol, 32 mg), 6-bromo-2-aminoquinoline (**30**, 50 mg, 0.22 mmol), K_2CO_3 (3 M aq, 100 μL, 0.3 mmol), PS-PPh_3-Pd (0.11 mmol/g, 2.2 μmol, 20 mg), and dimethoxyethane/EtOH (50%, 1 mL) was heated in microwave at 140 °C for 10 min. The resulting mixture was cooled, filtered, and purified by HPLC (10−60% CH_3CN/water modified with 0.1% TFA) to give 6-(thiophen-3-yl)quinolin-2-amine (0.012 g, 24% yield). ^{1}H NMR (400 MHz, MeOH) δ 8.39 (d, J = 9.5 Hz, 1H), 8.18 (d, J = 2.0 Hz, 1H), 8.14 (dd, J = 8.8, 2.0 Hz, 1H), 7.80−7.84 (m, 1H), 7.70 (d, J = 8.8 Hz, 1H), 1H, 7.55−7.61 (m, 2H), 7.09 (d, J = 9.5 Hz, 1H). MS (ESI, positive ion) m/z: 227 (M + 1).

6-Phenylquinolin-2-amine (33). Using phenylboronic acid and following the procedure used to prepare **32** gave **33**. ^{1}H NMR (400 MHz, methanol-d_4) δ 8.41 (d, J = 9.2 Hz, 1H), 8.14 (d, J = 2.0 Hz, 1H), 8.09 (dd, J = 8.7, 2.0 Hz, 1H), 7.69−7.78 (m, 3H), 7.48−7.55 (m, 2H), 7.38−7.46 (m, 1H), 7.10 (d, J = 9.2 Hz, 1H). MS (ESI, positive ion) m/z: 221 (M + 1).

6-*o*-Tolylquinolin-2-amine (34). Using *o*-tolylboronic acid and following the procedure used to prepare **32** gave **34**. ^{1}H NMR (400 MHz, methanol-d_4) δ 8.38 (d, J = 9.2 Hz, 1H), 7.82−7.87 (m, 1H), 7.75−7.81 (m, 1H), 7.72 (d, J = 8.6 Hz, 1H), 7.22−7.36 (m, 4H), 7.10 (d, J = 9.2 Hz, 1H), 2.28 (s, 3H). MS (ESI, positive ion) m/z: 235 (M + 1).

6-(2-Chlorophenyl)quinolin-2-amine (35). Using 2-chlorophenylboronic acid and following the procedure used to prepare **32** gave **35**. ^{1}H NMR (400 MHz, methanol-d_4) δ 8.40 (d, J = 9.4 Hz, 1H), 7.96 (d, J = 2.0 Hz, 1H), 7.89 (dd, J = 8.6, 2.0 Hz, 1H), 7.75 (d, J = 8.6 Hz),

1H, 7.55−7.61 (m, 1H), 7.40−7.50 (m, 3H), 7.12 (d, J = 9.4 Hz, 1H). MS (ESI, positive ion) m/z: 255, 257 (M + 1).

6-(3-Chlorophenyl)quinolin-2-amine (36). Using 3-chlorophenylboronic acid and following the procedure used to prepare **32** gave **36**. ^{1}H NMR (400 MHz, methanol-d_4) δ 8.43 (d, J = 9.4 Hz, 1H), 8.19 (d, J = 2.0 Hz, 1H), 8.10 (dd, J = 8.7, 2.0 Hz, 1H), 7.74−7.79 (m, 2H), 7.69 (dt, J = 7.7, 1.4 Hz, 1H), 7.51 (t, J = 7.7 Hz, 1H), 7.43−7.47 (m, 1H), 7.12 (d, J = 9.4 Hz, 1H). MS (ESI, positive ion) m/z: 255, 257 (M + 1).

6-(4-Chlorophenyl)quinolin-2-amine (37). Using 4-chlorophenylboronic acid and following the procedure used to prepare **32** gave **37**. ^{1}H NMR (400 MHz, methanol-d_4) δ 8.02 (d, J = 8.8 Hz, 1H), 7.91 (d, J = 2.0 Hz, 1H), 7.83 (dd, J = 8.8, 2.0 Hz, 1H), 7.69−7.73 (m, 2H), 7.62 (d, J = 8.8 Hz, 1H), 7.44−7.49 (m, 2H), 6.87 (d, J = 8.8 Hz, 1H). MS (ESI, positive ion) m/z: 255, 257 (M + 1).

6-Cyclohexylquinolin-2-amine (38). 6-Bromo-*N*-*tert*-butylquinolin-2-amine (1.21 g, 4.3 mmol, prepared as described in **28** but using 2-aminoquinolin-6-ol and *tert*-butylamine) and 1,1′-bis(diphenylphosphino)ferrocene-palladium(II)dichloride dichloromethane adduct (0.18 g, 0.22 mmol), was dissolved in dry tetrahydrofuran (50 mL) under nitrogen and cooled in an ice bath. Cyclohexylzinc bromide (0.5 M solution in THF, 11 mL, 5.4 mmol) was added. The reaction mixture was heated to 60 °C for 40 min. Then the solution was evaporated to dryness under reduced pressure. The crude material was purified by column chromatography on silica gel (eluting with a gradient of 0−50% ethyl acetate in hexane) to give *N*-*tert*-butyl-6-cyclohexylquinolin-2-amine (0.28 g, 23% yield).

N-*tert*-Butyl-6-cyclohexylquinolin-2-amine (0.28 g, 0.99 mmol) was dissolved in trifluoroacetic acid (30 mL) and heated to reflux. After 20 min, the solvent was evaporated to dryness under reduced pressure. The crude material was redissolved in dichloromethane (50 mL) and washed with saturated aqueous sodium bicarbonate (20 mL). The organic layer was separated, dried on sodium sulfate, filtered, and concentrated. The crude product was purified by column chromatography on silica gel (eluting with a gradient of 0−10% methanol in dichloromethane) to give 6-cyclohexylquinolin-2-amine (0.049 g, 22% yield). ^{1}H NMR (400 MHz, chloroform-*d*) δ 7.86 (d, J = 8.8 Hz, 1H), 7.62 (d, J = 8.6 Hz, 1H), 7.47 (dd, J = 8.6, 2.0 Hz, 1H), 7.42 (d, J = 2.0 Hz, 1H), 6.70 (d, J = 8.8 Hz, 1H), 5.15 (br s, 2H), 2.60 (m, 1H), 1.7−2.0 (m, 5 H), 1.2−1.6 (m, 5H). MS (ESI, positive ion) m/z: 227 (M + 1).

6-(2-(3,3-Dimethylbut-1-ynyl)phenyl)quinolin-2-amine (39). 6-Aminoquinoline (5.37 g, 37.2 mmol) was dissolved in 5N HCl (30 mL) and cooled in an ice bath. A solution of sodium nitrite (2.57 g, 37.2 mmol) in water (20 mL) was added slowly, and the mixture was stirred for 15 min. Ethyl acetate (200 mL) was added, followed by slow addition of a solution of sodium iodide (5.58 g, 37.2 mmol) in water (20 mL). After the reaction mixture was stirred for 10 min, the organic layer was separated and washed sequentially with water (200 mL), saturated sodium bicarbonate solution (100 mL), and finally sodium sulfite solution (100 mL). Then it was dried with magnesium sulfate, filtered, and concentrated. The crude material was purified by column chromatography on silica gel eluted with dichloromethane in hexane to give 6-iodoquinoline (4.65 g, 49.0% yield) as a yellow solid.

6-Iodoquinoline (0.39 g, 1.53 mmol), potassium carbonate (0.42 g, 3.05 mmol), 2-bromophenylboronic acid (0.32 g, 1.60 mmol), tetrakis-triphenylphosphine palladium(0) (0.088 g, 0.076 mmol), and ethanol (10 mL) were combined and heated to reflux under nitrogen for 2.5 h. The reaction mixture was concentrated to dryness. Then the crude material was dissolved in dichloromethane (40 mL) and washed with water (40 mL). The organic layer was separated, dried with magnesium sulfate, filtered, and concentrated. The crude material was purified by column chromatography on silica gel (eluting with a gradient of 50−100% dichloromethane in hexane) to give 6-(2-bromophenyl)quinoline (0.39 g, 90% yield).

6-(2-Bromophenyl)quinoline (0.39 g, 1.37 mmol) and *m*-chloroperoxybenzoic acid (0.81 g, 3.53 mmol) were dissolved in chloroform (30 mL) and heated to reflux. After 10 min, the reaction mixture was worked up with 1N sodium hydroxide (60 mL) and extracted with dichloromethane. The organic layer was dried with magnesium sulfate, filtered, and concentrated. The crude material was suspended in trifluoromethylbenzene (20 mL) and treated with *tert*-butylamine (1.0 mL, 9.51 mmol). Chloroform (3 mL) was added, followed by *p*-toluenesulfonic anhydride (0.58 g, 1.78 mmol, added in small portions). The reaction mixture was stirred for 10 min and then was worked up with sodium hydroxide (1N, 50 mL) and water (50 mL) and extracted with dichloromethane. The organic layer was separated, dried with magnesium sulfate, filtered, and concentrated. The crude material was purified with column chromatography on silica gel (eluting with a gradient of 0−100% dichloromethane in hexane) to give 6-(2-bromophenyl)-*N*-*tert*-butylquinolin-2-amine (0.31 g, 64% yield) as a colorless oil.

6-(2-Bromophenyl)-*N*-*tert*-butylquinolin-2-amine (0.31 g, 0.87 mmol) was dissolved in trifluoroacetic acid (40 mL) and heated to reflux for 90 min. The solvent was removed, and the residue was redissolved in dichloromethane and washed with 1N NaOH, water, and brine. The organic layer was separated, dried on sodium sulfate, filtered, and concentrated. The crude material was purified by column chromatography on silica gel (eluting with a gradient of 30−100% ethyl acetate in hexane) to give 6-(2-bromophenyl)quinolin-2-amine (0.26 g, 99% yield) as a white solid.

6-(2-Bromophenyl)quinolin-2-amine (0.24 g, 0.82 mmol) was dissolved in triethylamine (0.57 mL, 4.08 mmol) and dry DMF (1.5 mL) and transferred to a microwave vessel. Copper(I) iodide (7.8 mg, 0.041 mmol), dichlorobis(triphenylphosphine)palladium(II) (0.029 g, 0.041 mmol), and 3,3-dimethyl-1-butyne (0.15 mL, 1.22 mmol) were added, and the reaction was heated to 140 °C for 20 min. The crude mixture was partitioned between water (60 mL) and ethyl acetate (100 mL). The organic layer was dried with magnesium sulfate, filtered, and concentrated. The crude material was purified by column chromatography on silica gel (eluting with a gradient of 0−100% dichloromethane in ethyl acetate) to give enriched material, which was further purified using reverse phase HPLC to give 6-(2-(3,3-dimethylbut-1-ynyl)phenyl)quinolin-2-amine (0.065 g, 26% yield). ^{1}H NMR (400 MHz, chloroform-*d*) δ 7.87 (m, 3H), 7.68 (d, J = 8.4 Hz, 1H), 7.51 (dd, J = 7.6, 1.2 Hz, 1H) 7.44 (dd, J = 7.6, 1.2 Hz, 1H), 7.34 (td, J = 7.4 (×2), 1.6 Hz, 1H), 7.26 (ddd, J = 8.0, 7.0, 1.4 Hz, 1H), 6.73 (d, J = 8.8 Hz, 1H), 4.87 (br s, 2H), 1.15 (s, 9H). MS (ESI, positive ion) m/z: 301 (M + 1).

3-(2-Aminoquinolin-3-yl)-*N*-cyclohexyl-*N*-methylpropanamide (40). Quinoline-3-carboxaldehyde (1.0 g, 6.36 mmol) was dissolved in dry tetrahydrofuran (30 mL) and treated with methyl (triphenylphosphoranylidene) acetate (2.13 g, 6.36 mmol). The reaction was heated to 60 °C for 90 min. Then the solvent was removed under reduced pressure. The crude material was purified by column chromatography on silica gel (eluting with a gradient of 0−30% ethyl acetate in dichloromethane) to give the methyl 3-(quinolin-3-yl)acrylate as a white solid. This material was dissolved in methanol (60 mL) and treated with a solution of lithium hydroxide monohydrate (1.33 g, 31.8 mmol) in water (30 mL). The solution was heated to 50 °C and stirred for 40 min. The reaction mixture was neutralized with 5N hydrochloric acid (6.5 mL), and the solvent was removed to dryness under reduced pressure. The crude material was dried under high vacuum with heat to remove remaining residual water. The crude 3-(quinolin-3-yl)acrylic acid was suspended in thionyl chloride (85 mL, 1.17 mol) and heated to 80 °C for 90 min. The reaction mixture was evaporated to dryness under reduced pressure and further dried under high vacuum. Dichloromethane (80 mL) was added, and a solution of diisopropylethylamine (3.5 mL, 20 mmol) and *N*-methylcyclohexylamine (1.0 mL, 7.8 mmol) in dichloromethane (80 mL) was added. The suspension was stirred for 10 min. Then water (100 mL) and ethyl acetate (100 mL) were added. The organic layer was separated, dried on sodium sulfate, filtered, and concentrated. The crude material was purified by column chromatography on silica gel (eluting with a

gradiet of 0−100% ethyl acetate in dichloromethane) to give *N*-cyclohexyl-*N*-methyl-3-(quinolin-3-yl)acrylamide (1.38 g, 72% yield over 3 steps).

N-Cyclohexyl-*N*-methyl-3-(quinolin-3-yl)acrylamide (0.29 g, 0.98 mmol) was dissolved in methanol (20 mL) and treated with palladium on carbon (0.052 g, 0.049 mmol). The reaction mixture was stirred under a hydrogen balloon for 3 h then filtered through a pad of Celite, and the filtrate was evaporated to dryness under reduced pressure. The crude material was dissolved in chloroform (20 mL) and treated with *m*-chloroperoxybenzoic acid (0.45 g, 1.95 mmol). The solution was heated to reflux for 60 min. 1N Sodium hydroxide (50 mL) and dichloromethane (50 mL) were added. The organic layer was separated, dried with magnesium sulfate, filtered, and concentrated. The crude material was dissolved in a mixture of trifluoromethylbenzene (20 mL) and *tert*-butylamine (0.80 mL, 7.61 mmol) prior to addition of *p*-toluenesulfonic anhydride (0.45 g, 1.36 mmol). The reaction mixture was stirred for 15 min. Then water (20 mL), 1N sodium hydroxide (30 mL), and dichloromethane (60 mL) were added. The organic layer was separated and washed with additional 1N sodium hydroxide (50 mL), then dried with magnesium sulfate, filtered, and concentrated. The crude material was purified by column chromatography on silica gel (eluting with a gradient of 0−100% ethyl acetate in hexane) to give 3-(2-(*tert*-butylamino)quinolin-3-yl)-*N*-cyclohexyl-*N*-methylpropanamide (0.16 g, 45% yield).

3-(2-(*tert*-Butylamino)-6-*o*-tolylquinolin-3-yl)-*N*-cyclohexyl-*N*-methylpropanamide (0.090 g, 0.24 mmol) was dissolved in trifluoroacteic acid (40 mL) and heated to reflux for 30 min. The solvent was removed under reduced pressure. The crude material was added dichloromethane (15 mL) and saturated sodium bicarbonate aqueous solution (20 mL). The organic layer was separated, dried on sodium sulfate, filtered, and concentrated. The crude material was purified by column chromatography on silica gel (eluting with a gradient of 0−10% methanol in dichloromethane) to give 3-(2-amino-6-*o*-tolylquinolin-3-yl)-*N*-cyclohexyl-*N*-methylpropanamide (0.025 g, 33% yield). ^{1}H NMR (400 MHz, chloroform-*d*) δ 8.70 (br s, 2H), 7.86 (d, J = 3.1 Hz, 1H), 7.76 (d, J = 8.4 Hz, 1H), 7.59 (m, 2H), 7.33 (t, J = 7.5 Hz, 1H), 3.05−3.15 (m, 2H), 2.82 (s, 3H, 3:2 mix of rotomers), 2.74 (t, J = 6.3 Hz, 1H), 2.69 (t, J = 6.3 Hz, 1H) 1.00−1.89 (m, 11H). MS (ESI, positive ion) m/z: 312 (M + 1).

3-(2-Amino-6-*o*-tolylquinolin-3-yl)-*N*-cyclohexyl-*N*-methylpropanamide (41). 2-Amino-5-bromobenzaldehyde (2.6 g, 13.0 mmol) was dissolved in toluene (100 mL) and treated with methyl 3,3-dimethoxypropionate (1.84 mL, 13.0 mmol). *p*-Toluenesulfonic acid monohydrate (0.25 g, 1.30 mmol) was added, and the solution was heated to reflux with a Dean−Stark trap for 90 min. The solvent was removed under reduced pressure. The crude material was added ethyl acetate (300 mL), water (100 mL), and saturated sodium bicarbonate aqueous solution (20 mL). The organic layer was separated, dried with magnesium sulfate, filtered, and concentrated to give the crude methyl 6-bromoquinoline-3-carboxylate (3.2 g, 93% yield) as a yellow solid. This material was used without further purification.

Methyl 6-bromoquinoline-3-carboxylate (0.99 g, 3.71 mmol), potassium carbonate (2.05 g, 14.8 mmol), *o*-tolylboronic acid (0.96 g, 7.05 mmol), and tetrakis(triphenylphosphine)palladium(0) (0.24 g, 0.21 mmol) were suspended in ethanol (5 mL) and heated in the microwave to 120 °C for 10 min. The crude mixture was partitioned between water (100 mL) and ethyl acetate (100 mL). The organic layer was separated, dried with magnesium sulfate, filtered, and concentrated. The crude material was purified by column chromatography on silica gel (eluting with a gradient of 0−100% ethyl acetate in hexane) to give methyl 6-*o*-tolylquinoline-3-carboxylate. This material was dissolved in dichloromethane (40 mL) and cooled in an ice bath under nitrogen. Diisobutylaluminum hydride (1.0 M solution in hexanes, 3.71 mL, 3.71 mmol) was added, and the solution was stirred for 90 min. Then methanol (10 mL) and saturated ammonium chloride aqueous solution (10 mL) were carefully added. The mixture was stirred for 15 min, and then ethyl acetate (100 mL) and water (100 mL) were added. The organic layer was separated, dried with magnesium sulfate, filtered, and concentrated. The crude material was purified by column chromatography on silica gel (eluting with a gradient of 0−10% methanol in dichloromethane) to give (6-*o*-tolylquinolin-3-yl)methanol (0.22 g, 24% yield for 2 steps).

(6-*o*-Tolylquinolin-3-yl)methanol (0.22 g, 0.88 mmol) was dissolved in dichloromethane (50 mL) and treated with tetrapropylammonium perruthenate (0.016 g, 0.044 mmol) and 4-methylmorpholine 4-oxide (0.16 g, 1.32 mmol). The reaction was stirred for 60 min. The crude mixture was concentrated under reduced pressure to ∼10 mL and passed through a pad of silica eluting with ethyl acetate to give 6-*o*-tolylquinoline-3-carbaldehyde (0.094 g, 44% yield). This material was dissolved in dry tetrahydrofuran (20 mL) and treated with methyl (triphenylphosphoranylidene) acetate (0.20 g, 0.60 mmol). The reaction mixture was stirred at room temperature for 20 min. The solvent was removed, and the crude material was purified by column chromatography on silica gel (eluting with a gradient of 0−100% ethyl acetate in hexane) to give methyl 3-(6-*o*-tolylquinolin-3-yl)acrylate. This material was dissolved in methanol (30 mL) and treated with a solution of lithium hydroxide monohydrate (0.048 g, 1.15 mmol) in water (5 mL). The solution was stirred for 40 min, and then 5N hydrochloric acid (0.5 mL) was added. The mixture was evaporated to dryness under reduced pressure and the crude solid further dried under high vacuum. The crude material was suspended in excess thionyl chloride (20 mL) and heated to reflux for 30 min. Then the reaction mixture was concentrated to dryness and further dried under high vacuum. The residue was dissolved in dichloromethane (20 mL) and treated with *N*-methylcyclohexylamine (0.30 mL, 2.27 mmol). After 15 min, the solution was evaporated to dryness under reduced pressure and the crude material was purified by column chromatography on silica gel (eluting with a gradient of 0−100% ethyl acetate in hexane). The product was further purified by reverse phase HPLC to give *N*-cyclohexyl-*N*-methyl-3-(6-*o*-tolylquinolin-3-yl)acrylamide (0.15 g, 43% yield).

The *N*-cyclohexyl-*N*-methyl-3-(6-*o*-tolylquinolin-3-yl)acrylamide (0.1 g, 0.38 mmol) was dissolved in methanol (80 mL) and treated with palladium on activated carbon (10% by weight, 0.041 g, 0.039 mmol). The solution was stirred under hydrogen for 30 min. Then the mixture was filtered through a pad of Celite. The filtrate was evaporated to dryness under reduced pressure. The crude material was purified by column chromatography on silica gel (eluting with a gradient of 0−100% ethyl acetate in dichloromethane) to give *N*-cyclohexyl-*N*-methyl-3-(6-*o*-tolylquinolin-3-yl)propanamide. This material was dissolved in chloroform (20 mL) and treated with *m*-chloroperoxybenzoic acid (0.10 g, 0.58 mmol). The solution was heated to reflux for 10 min then diluted with dichloromethane (30 mL) and washed with 1N sodium hydroxide (70 mL). The organic was dried with magnesium sulfate and evaporated to dryness under reduced pressure. This material was combined with trifluoromethylbenzene (20 mL) and *tert*-butylamine (0.20 mL, 1.9 mmol). Then *p*-toluenesulfonic anhydride (0.15 g, 0.46 mmol) was added in small portions. The mixture was stirred for 20 min. Then water (100 mL), 5N sodium hydroxide (30 mL), and dichloromethane (70 mL) were added. The organic layer was separated, dried with magnesium sulfate, filtered, and concentrated. The crude material was purified by column chromatography on silica gel (eluting with a gradient of 0−100% ethyl acetate in hexane) to give 3-(2-(*tert*-butylamino)-6-*o*-tolylquinolin-3-yl)-*N*-cyclohexyl-*N*-methylpropanamide (0.090 g, 51% yield).

3-(2-(*tert*-Butylamino)-6-*o*-tolylquinolin-3-yl)-*N*-cyclohexyl-*N*-methylpropanamide (0.090 g, 0.20 mmol) was dissolved in trifluoroacetic acid (40 mL) and heated to reflux for 20 min. The solvent was removed, and the residue was taken in dichloromethane (15 mL) and saturated sodium bicarbonate solution (20 mL). The organic layer was separated, dried on sodium sulfate, filtered, and concentrated. The crude material was

purified by column chromatography on silica gel (eluting with a gradient of 0−10% methanol in dichloromethane) to give 3-(2-amino-6-*o*-tolylquinolin-3-yl)-*N*-cyclohexyl-*N*-methylpropanamide (0.025 g, 32% yield). ^{1}H NMR (400 MHz, chloroform-*d*) δ 7.74 (m, 2H), 7.52 (m, 2H), 7.28(m, 4H), 6.62 (br s, 2H), 3.08 (m, 2H), 2.82 (s, 3H, mix of rotomers), 2.76 (t, J = 6.5 Hz, 1H), 2.70 (t, J = 6.5 Hz, 1H), 2.28 (s, 3H), 0.9−1.9 (m, 11H). MS (ESI, positive ion) m/z: 402.2 (M + 1).

3-(2-Amino-6-*o*-tolylquinolin-3-yl)-*N*-cyclohexylpropanamide (42). Using cyclohexanamine and following the procedure used to prepare **41** gave **42**. ^{1}H NMR (300 MHz, chloroform-*d*) δ ppm 0.95−1.15 (m, 3H) 1.27−1.41 (m, 2H) 1.52−1.72 (m, 3H) 1.86 (dd, J = 12.35, 3.43 Hz, 2H) 2.29 (s, 3H) 2.54 (t, J = 6.87 Hz, 2H) 3.01 (t, J = 6.80 Hz, 2H) 3.68−3.84 (m, 1H) 5.28−5.38 (m, 1H) 5.43 (br s, 2H) 7.28 (s, 4 H) 7.46−7.54 (m, 2H) 7.63−7.73 (m, 2H). MS (ESI, positive ion) m/z: 388.2 (M + 1).

3-(2-Amino-6-*o*-tolylquinolin-3-yl)-*N*-(cyclohexylmethyl)propanamide (43). Using cyclohexylmethanamine and following the procedure used to prepare **41** gave **43**. ^{1}H NMR (300 MHz, chloroform-*d*) δ ppm 0.69−0.93 (m, 2H) 0.99−1.22 (m, 3H) 1.36 (br s, 1H) 1.48−1.74 (m, 5H) 2.29 (s, 3 H) 2.57 (t, J = 6.80 Hz, 2H) 2.89−3.16 (m, 4H) 5.62 (br s, 1H) 5.75 (br s, 1H) 7.20−7.36 (m, 4H) 7.43−7.56 (m, 2H) 7.61−7.79 (m, 2H). MS (ESI, positive ion) m/z: 402.2 (M + 1).

3-(2-Aminoquinolin-3-yl)-*N*-(cyclohexylmethyl)propanamide (44). Using cyclohexylmethanamine and following the procedure used to prepare **41** gave **44**. ^{1}H NMR (400 MHz, chloroform-*d*) δ 7.66 (s, 1H), 7.63 (d, J = 8.4 Hz, 1H), 7.55 (d, J = 8 Hz, 1H), 7.50 (ddd, J = 8.4, 7.0, 1.5 Hz, 1H), 7.22 (td, J = 7.5, 7.5, 1.1, 1H), 5.61 (br s, 1H), 5.29 (br s, 2H), 3.05 (t, J = 6.4 Hz, 2H), 2.98 (t, J = 6.9 Hz, 2H), 2.54 (t, J = 7.0 Hz, 2H), 1.50−1.70 (m, 5H), 1.0−1.45 (m, 4H), 0.7−0.9 (m, 2H). MS (ESI, positive ion) m/z: 312 (M + 1).

3-(2-Amino-6-*o*-tolylquinolin-3-yl)-*N*-(cyclohexylmethyl)-2-methylpropanamide (45). (6-*o*-Tolylquinolin-3-yl)methanol (0.32 g, 1.28 mmol, prepared as in **41**) was dissolved in toluene (50 mL) and treated with manganese dioxide (0.33 g, 3.83 mmol). The mixture was heated to reflux for 80 min. The reaction mixture was filtered through a pad of Celite into a suspension of triethyl 2-phosphonopropionate (0.33 mL, 1.53 mmol) and potassium *t*-butoxide (0.18 g, 1.59 mmol) in dry tetrahydrofuran (20 mL). The resulting solution was stirred for 45 min. The solvent was removed, and the crude material was purified by column chromatography on silica gel (eluting with a gradient of 0−100% ethyl acetate in hexane) to give ethyl 2-methyl-3-(6-*o*-tolylquinolin-3-yl)acrylate (0.27 g, 64% yield).

Ethyl 2-methyl-3-(6-*o*-tolylquinolin-3-yl)acrylate (0.27 g, 0.82 mmol) was dissolved in methanol (50 mL) and treated with a solution of lithium hydroxide monohydrate (0.34 g, 8.21 mmol) in water (10 mL). The reaction mixture was stirred for 30 min, and then 5N hydrochloric acid (1.8 mL) was added. The solvent was removed, and the material was dried on high vacuum. To this material, thionyl chloride (30 mL, 411 mmol) was added and the mixture was heated to reflux for 30 min. The solvent was removed, and the residue was resuspended in dichloromethane and once again evaporated to dryness under reduced pressure and further dried under high vacuum. This material was dissolved in dichloromethane (30 mL) and treated with aminomethylcyclohexane (0.40 mL, 3.08 mmol) and diisopropylethylamine (1.0 mL, 5.74 mmol). The reaction mixture was stirred for 45 min. Water (100 mL) and ethyl acetate (100 mL) were added, and the organic layer was separated, dried with magnesium sulfate, filtered, and concentrated. The crude material was purified by column chromatography on silica gel (eluting with a gradient of 0−100% ethyl acetate in hexane) to give the *N*-(cyclohexylmethyl)-2-methyl-3-(6-*o*-tolylquinolin-3-yl)acrylamide (0.29 g, 89% yield over three steps).

N-(Cyclohexylmethyl)-2-methyl-3-(6-*o*-tolylquinolin-3-yl)acrylamide (0.29 g, 0.73 mmol) was dissolved in methanol (50 mL), treated with palladium on carbon (10%, 0.085 g), and stirred under hydrogen for 3 h. The reaction mixture was filtered through a pad of Celite, and the filtrate was evaporated to dryness under reduced pressure. The crude product was dissolved in chloroform (30 mL) and treated with 3-chloroperoxybenzoic acid (0.17 g, 1.01 mmol). The solution was heated to reflux for 60 min. Then dichloromethane (80 mL) and 1N sodium hydroxide (100 mL) were added, and the organic layer was separated, dried with magnesium sulfate, filtered, and concentrated. This material was dissolved in a mixture of trifluoromethylbenzene (10 mL) and *tert*-butylamine (0.50 mL, 4.76 mmol) and treated with *p*-toluenesulfonic anhydride (0.26 g, 0.81 mmol). The reaction mixture was stirred for 40 min, and then dichloromethane (70 mL) and 1N sodium hydroxide (50 mL) were added. The organic layer was separated, dried with magnesium sulfate, filtered, and concentrated. The crude material was purified by column chromatography on silica gel (eluting with a gradient of 0−30% ethyl acetate in hexane) to give 3-(2-(*tert*-butylamino)-6-*o*-tolylquinolin-3-yl)-*N*-(cyclohexylmethyl)-2-methylpropanamide (0.14 g, 45% yield).

3-(2-(*tert*-Butylamino)-6-*o*-tolylquinolin-3-yl)-*N*-(cyclohexylmethyl)-2-methylpropanamide (0.14 g, 0.30 mmol) was dissolved in trifluoroacetic acid (20 mL) and heated to reflux for 20 min. The solvent was removed, and the residue was taken in 1N NaOH and extracted with dichloromethane. The organic layer was separated, dried on sodium sulfate, filtered, and concentrated. The crude material was purified by column chromatography on silica gel (eluting with a gradient of 0−10% methanol in dichloromethane) to give 3-(2-amino-6-*o*-tolylquinolin-3-yl)-*N*-(cyclohexylmethyl)-2-methylpropanamide (0.052 g, 19% yield). ^{1}H NMR (400 MHz, methanol-d_4) δ 7.79 (s, 1H), 7.64 (d, J = 8.4 Hz, 1H), 7.53 (m, 2H), 7.43 (s, 1H), 7.27 (m, 4H), 4.24 (br s, 3H), 3.04 (m, 2H), 2.73 (m, 3H), 2.28 (s, 3H), 1.1−1.6 (m, 9H), 0.6−1.0 (m, 5H). MS (ESI, positive ion) m/z: 416 (M + 1).

(*R*)-3-(2-Amino-6-*o*-tolylquinolin-3-yl)-*N*-(cyclohexylmethyl)-2-methylpropanamide (46) and (*S*)-3-(2-Amino-6-*o*-tolylquinolin-3-yl)-*N*-(cyclohexylmethyl)-2-methylpropanamide (47). Chiral purificaton of 3-(2-amino-6-*o*-tolylquinolin-3-yl)-*N*-(cyclohexylmethyl)-2-methylpropanamide (**45**) was performed with preparative supercritical fluid chromatography (SFC) by Lotus Separations: Chiralpak IA (3 cm × 15 cm) column; mobile phase, 20% methanol (0.2% EDA)/CO_2, 100 bar; flow rate = 80 mL/min; 220 nm; 0.5 mL injection with 25 mg/10 mL in methanol. The resulting **46** and **47** have ee values of >98% and >99%, respectively, according to Lotus.

2-((2-Amino-6-*o*-tolylquinolin-3-yl)methyl)-*N*-(cyclohexylmethyl)butanamide (48). Using ethyl 2-(diethoxyphosphoryl)-butanoate and following the procedure used to prepare **45** gave **48**. ^{1}H NMR (400 MHz, chloroform-*d*) δ 7.69 (s, 1H), 7.63 (d, J = 8.4 Hz, 1H), 7.47 (m, 2H), 7.26 (m, 4H), 5.68 (br s, 1H), 5.31 (br s, 2H), 3.04 (m, 2H), 2.87 (m, 1H), 2.68 (dd, J = 14.3, 4.3 Hz, 1H), 2.36 (m, 1H), 2.28 (s, 3H), 1.1−1.9 (m, 9H), 0.85−1.0 (m, 5H), 0.55−0.70 (m, 2H). MS (ESI, positive ion) m/z: 430 (M + 1).

2-((2-Amino-6-*o*-tolylquinolin-3-yl)methyl)-*N*-(cyclohexylmethyl)-3-methylbutanamide (49). Using ethyl 2-(diethoxyphosphoryl)-3-methylbutanoate and following the procedure used to prepare **45** gave **49**. ^{1}H NMR (400 MHz, chloroform-*d*) δ 7.69 (m, 2H), 7.49 (m, 2H), 7.26 (m, 4H), 5.22 (br m, 3H), 3.04 (m, 2H), 2.81 (m, 2H), 2.29 (s, 3H), 2.06 (m, 2H), 0.8−1.65 (m, 15H), 0.59 (m, 2H). MS (ESI, positive ion) m/z: 444 (M + 1).

2-((2-Amino-6-*o*-tolylquinolin-3-yl)methyl)-*N*-(cyclohexylmethyl)pentanamide (50). Using ethyl 2-(diethoxyphosphoryl)-pentanoate and following the procedure used to prepare **45** gave **50**. ^{1}H NMR (400 MHz, chloroform-*d*) δ 7.79 (s, 1H), 7.69 (m, 1H), 7.53 (m, 2H), 7.27 (m, 4H), 6.12 (br s, 2H), 5.89 (br s, 1H), 3.07 (m, 2H), 2.89 (m, 1H), 2.75 (dd, J = 14.5, 4.9 Hz, 1H), 2.52 (m, 1H), 2.28 (s, 3H), 1.78 (m, 1H), 1.1−1.6 (m, 9H), 0.8−1.0 (m, 6H), 0.6−0.8 (m, 2H). MS (ESI, positive ion) m/z: 444 (M + 1).

(*R*)-3-(2-Amino-6-*o*-tolylquinolin-3-yl)-*N*-(3,3-dimethylbutyl)-2-methylpropanamide (51). Using 3,3-dimethylbutan-1-amine and following the procedure used to prepare **45** afforded 3-(2-Amino-6-*o*-tolylquinolin-3-yl)-*N*-(3,3-dimethylbutyl)-2-methylpropanamide. Chiral purificaton of the racemic material via preparative SFC afforded (*S*)- and (*R*)-3-(2-amino-6-*o*-tolylquinolin-3-yl)-*N*-(3,3-dimethylbutyl)-2-methylpropanamide: Chiralcel OJ-H (250 mm × 21 mm, 40 °C, 5 μm) column; mobile phase, 88:12 (A:B), A = liquid CO_2, B = methanol (0.2% DEA); 100 bar; flow rate = 62 mL/min; 252 nm. The resulting enantiomers have ee values of 99.98% and >99%, respectively. ^{1}H NMR (300 MHz, chloroform-*d*) δ ppm 0.82 (s, 9H) 1.12−1.23 (m, 2H) 1.30 (d, *J* = 6.72 Hz, 3H) 2.30 (s, 3H) 2.48−2.60 (m, 1H) 2.60−2.72 (m, 1H) 3.05−3.23 (m, 3H) 5.16−5.26 (m, 2H) 5.28−5.35 (m, 1H) 7.27 (t, *J* = 1.53 Hz, 4H) 7.47−7.55 (m, 2H) 7.68 (d, *J* = 1.17 Hz, 2H). MS (ESI, positive ion) *m*/*z*: 404.1 (M + 1).

(*R*)-3-(2-Amino-6-*o*-tolylquinolin-3-yl)-*N*-benzyl-2-methylpropanamide (52). Using benzylamine and following the procedure used to prepare **45** afforded 3-(2-amino-6-*o*-tolylquinolin-3-yl)-*N*-benzyl-2-methylpropanamide. Chiral purification of the racemic material via preparative SFC: OJH (250 mm × 21 mm, 5 μm) column; mobile phase 27% methanol (0.2% DEA)/CO_2; flow rate = 65 mL/min; 220 nm; 100 bar. The resulting (*S*)- and (*R*)-3-(2-amino-6-*o*-tolylquinolin-3-yl)-*N*-benzyl-2-methylpropanamide have ee values of 100%, respectively. ^{1}H NMR (300 MHz, chloroform-*d*) δ ppm 1.35 (d, *J* = 6.72 Hz, 3H) 2.30 (s, 3H) 2.58−2.64 (m, 1H) 2.64−2.76 (m, 1H) 3.06−3.24 (m, 1H) 4.22−4.50 (m, 2H) 5.14−5.27 (m, 2H) 5.61−5.72 (m, 1H) 6.95−7.02 (m, 2H) 7.15 (s, 3 H) 7.27−7.31 (m, 4H) 7.47−7.50 (m, 1H) 7.50−7.56 (m, 1H) 7.71 (s, 2H). MS (ESI, positive ion) *m*/*z*: 410.0 (M + 1).

3-(2-Amino-6-*o*-tolylquinolin-3-yl)-2-methyl-*N*-(pyridin-3-ylmethyl)propanamide (53). *N*,*N*-Dimethylformamide (54 mL, 0.70 mol) was added dropwise (via a syringe pump) to phosphoryl trichloride (179 mL, 1.96 mol) in a 350 mL sealed tube in an ice bath under nitrogen. After the addition, the water bath was removed and *N*-(4-bromophenyl)acetamide (60 g, 0.28 mol) was added in one portion and stirred until a homogeneous solution was observed (approximately 30 min.). The reaction vessel was sealed and heated at 75 °C for 48 h. The reaction was allowed to cool and slowly poured onto ice (final volume of 2 L) and stirred for 25 min. The solid was filtered and washed with water until the filtrate was no longer acidic (∼3 L) and the product was dried in an oven vacuum overnight at 50 °C to afford 6-bromo-2-chloroquinoline-3-carbaldehyde as a light-tan colored solid (45.7 g, 60% yield).

6-Bromo-2-chloroquinoline-3-carbaldehyde (10 g, 0.37 mol) and 4-methoxybenzylamine (144 mL, 1.11 mol) in EtOH (200 mL) was heated at 125 °C in a sealed tube for 2.5 h. The reaction mixture was cooled and poured into 1N HCl (200 mL) and stirred 2 h. The mixture was extracted with chloroform, and the combined organic layers was washed with 1N HCl and brine, dried over sodium sulfate, filtered, and concentrated to afford 2-(4-methoxybenzylamino)-6-bromoquinoline-3-carbaldehyde (12.4 g, 91% yield).

Lithium chloride (2.41 g, 56.7 mmol) was stirred 4 h in MeCN (300 mL). To the cloudy solution was added 2-(4-methoxybenzylamino)-6-bromoquinoline-3-carbaldehyde (10.5 g, 28.4 mmol), ethyl 2-(diethoxyphosphoryl)propanoate (7.4 mL, 34.0 mmol), and 2,3,4,6,7,8,9,10-octahydropyrimido[1,2-*a*]azepine (4.3 mL, 28.4 mmol), and the reaction was stirred 12 h. The reaction was partitioned between 10% sodium carbonate solution and ethyl acetate. The aqueous layer was extracted with ethyl acetate, and the combined organic layers were washed with 10% sodium carbonate aqueous solution, brine, dried over sodium sulfate, filtered, and concentrated. The crude mixture was purified by silica gel chromatography eluted with a gradient of 4:1 hexanes/EtOAc to afford ethyl 3-(2-(4-methoxybenzylamino)-6-bromoquinolin-3-yl)-2-methylacrylate (8.59 g, 67% yield).

1N LiOH (10.0 mL, 10.0 mmol) was added to a solution of ethyl 3-(2-(4-methoxybenzylamino)-6-bromoquinolin-3-yl)-2-methylacrylate (3.6 g, 7.9 mmol) in MeOH (10 mL) and THF (30 mL) at room temperature. The reaction was stirred 1 h before the organic solvent was removed and the remaining aqueous was brought to pH 1 with 1N HCl. The resulting suspension was extracted with a 2:1 chloroform/*i*-PrOH mixture. The combined organic layers were washed with brine, dried over sodium sulfate, and concentrated to afford 3-(2-(4-methoxybenzylamino)-6-bromoquinolin-3-yl)-2-methylacrylic acid, which was used without further purification (2.4 g, 71% yield).

A mixture of 3-(2-(4-methoxybenzylamino)-6-bromoquinolin-3-yl)-2-methylacrylic acid (0.10 g, 0.23 mmol), 3-(aminomethyl)pyridine (0.048 mL, 0.47 mmol), and *N*-ethyl-*N*-isopropylpropan-2-amine (0.091 mL, 0.53 mmol) were added followed by addition of *O*-(benzotriazol-1-yl)-*N*,*N*,*N*′,*N*′-tetramethyluronium tetra fluoroborate (TBTU, 0.098 g, 0.30 mmol) in NMP (2 mL), which was stirred at room temperature for 1 h. The mixture was quenched with saturated aqueous $NaHCO_3$ solution and stirred for 15 min. The mixture was poured into water and extracted with EtOAc. The combined organic layers were dried over Na_2SO_4, filtered, concentrated, and chromatographed on silica gel using a gradient of 0−75% ethyl acetate/hexane to afford 3-(2-(4-methoxybenzylamino)-6-bromoquinolin-3-yl)-2-methyl-*N*-(pyridin-3-ylmethyl)acrylamide (0.12 g, 99% yield)

A mixture of 3-(2-(4-methoxybenzylamino)-6-bromoquinolin-3-yl)-2-methyl-*N*-(pyridin-3-ylmethyl)acrylamide (0.12 g, 0.23 mmol), bis-(4-(di-*tert*-butylphosphino)-*N*,*N*-dimethylbenzenamine) dichloropalladium(II) (0.0025 g, 0.0035 mmol), *o*-tolylboronic acid (0.047 g, 0.35 mmol), and potassium acetate (0.046 g, 0.46 mmol) in EtOH (10 mL) and water (1 mL) was heated at 85 °C for 3 h. The mixture was concentrated and chromatographed on silica gel using 0−75% ethyl acetate/hexane to afford 3-(2-(4-methoxybenzylamino)-6-*o*-tolylquinolin-3-yl)-2-methyl-*N*-(pyridin-3-ylmethyl)acrylamide (0.10 g, 82% yield).

A mixture of 3-(2-(4-methoxybenzylamino)-6-*o*-tolylquinolin-3-yl)-2-methyl-*N*-(pyridin-3-ylmethyl)acrylamide (0.10 g, 0.2 mmol) and palladium on carbon (0.10 g, 0.9 mmol) in EtOH (20 mL) was stirred under a hydrogen balloon for 4 h. Then the mixture was filtered through a pad of Celite, and the filtrate was concentrated. The resulting material was added trifluoroacetic acid (7 mL) and heated at 63 °C for 1 h. The reaction mixture was concentrated and chromatographed on silica gel using a gradient of 0−3% 2 M NH_3 in MeOH/dichloromethane to afford 3-(2-amino-6-*o*-tolylquinolin-3-yl)-2-methyl-*N*-(pyridin-3-ylmethyl)propanamide (0.037 g, 48% yield). ^{1}H NMR (300 MHz, chloroform-*d*) δ 1.31 (d, *J* = 6.58 Hz, 3H), 2.27 (s, 3H), 2.62−2.77 (m, 2H), 3.06−3.18 (m, 1H), 3.47 (s, 1H), 4.20 (dd, *J* = 1.00 Hz, 1H), 4.40 (dd, *J* = 14.98, 6.36 Hz, 1H), 5.85 (br s, 1H), 6.84−6.97 (m, 2H), 7.16−7.33 (m, 5H), 7.44−7.56 (m, 2H), 7.65 (d, *J* = 8.62 Hz, 1H), 7.72 (s, 1H), 8.23 (d, *J* = 1.75 Hz, 1H), 8.29 (dd, *J* = 4.82, 1.32 Hz, 1H). MS (ESI, positive ion) *m*/*z*: 411 (M + 1).

3-(2-Amino-6-*o*-tolylquinolin-3-yl)-2-methyl-*N*-(thiazol-5-ylmethyl)propanamide (54). 6-Bromo-2-chloroquinoline-3-carbaldehyde (10 g, 37 mmol, prepared as in **53**) was dissolved in NMP 200 mL in a 350 mL sealable flask. *tert*-Butylamine (23 mL, 222 mmol) was added, and the reaction mixture was sealed and heated at 130 °C for 24 h. After cooling, the mixture was poured into 1N HCl 200 mL and stirred for 1.5 h. The precipitate was isolated by filtration and washed with water. The solid was collected and dried on vacuum pump overnight to give 2-(*tert*-butylamino)-6-bromoquinoline-3-carbaldehyde (10.4 g, 92% yield).

Lithium chloride (1.4 g, 33 mmol) was stirred overnight in acetonitrile (150 mL). To the cloudy solution was added 6-bromo-2-(*tert*-butylamino)quinoline-3-carbaldehyde (5.0 g, 16 mmol), ethyl 2-(diethoxyphosphoryl)propanoate (4.3 mL, 20 mmol), and 1,8-diazabicyclo-[5.4.0]undec-7-ene (2.4 mL, 16 mmol). The reaction mixture was stirred at room temperature for 10 h. To the reaction was added saturated

sodium bicarbonate solution and extracted with EtOAc three times. The combined organic layers were washed with brine and dried on sodium sulfate, filtered, and concentrated. The crude material was purified by column chromatography with a gradient of 30−60% dichloromethane/hexane to give ethyl 3-(6-bromo-2-(*tert*-butylamino)quinolin-3-yl)-2-methylacrylate (5.4 g, 85% yield).

Ethyl 3-(6-bromo-2-(*tert*-butylamino)quinolin-3-yl)-2-methylacrylate (4.43 g, 11 mmol), *o*-tolylboronic acid (2 g, 17 mmol), bis(4-(di-*tert*-butylphosphino)-*N*,*N*-dimethylbenzenamine) dichloropalladium-(II) (0.2 g, 0.2 mmol), potassium acetate (2 g, 23 mmol), and water (4 mL, 226 mmol) were combined in EtOH 100 mL and heated at 80 °C for 2 h. Then the solvent was removed, and the crude material was taken in saturated sodium bicarbonate solution and extracted with EtOAc. The combined organic layers were washed with brine, dried on sodium sulfate, filtered, and concentrated. The crude material was purified by column chromatography with a gradient of 0−100% ethyl acetate/hexane gradient to give ethyl 3-(2-(*tert*-butylamino)-6-*o*-tolylquinolin-3-yl)-2-methylacrylate. This material was dissolved in methanol, and Pd/C (2.0 g) was added. The reaction mixture was stirred under a hydrogen balloon overnight. Then the mixture was filtered through a pad of Celite. The filtrate was collected and concentrated. The crude material was purified by column chromatography with 40−60% dichloromethane/hexane gradient to give ethyl 3-(2-(*tert*-butylamino)-6-*o*-tolylquinolin-3-yl)-2-methylpropanoate (4.2 g, 92% yield)

Ethyl 3-(2-(*tert*-butylamino)-6-*o*-tolylquinolin-3-yl)-2-methylpropanoate (4.2 g, 10 mmol) was dissolved in MeOH 150 mL and 1N sodium hydroxide (42 mL, 42 mmol) was added. The reaction mixture was refluxed for 2 h and then cooled to room temperature. Then 5N HCl was added to neutralize the solution to pH 2−3. The solvent was removed, and the residue was taken in 1N HCl and extracted with dichlormethane three times. The combined organic layers were washed with water and brine, dried on sodium sulfate, filtered, and concentrated to give 3-(2-(*tert*-butylamino)-6-*o*-tolylquinolin-3-yl)-2-methylpropanoic acid (3.72 g, 94% yield).

3-(2-(*tert*-Butylamino)-6-*o*-tolylquinolin-3-yl)-2-methylpropanoic acid (0.077 g, 0.2 mmol) was dissolved in dichloromethane 1 mL. Thiazol-5-ylmethanamine hydrochloride (0.03 g, 0.2 mmol) was added, followed by addition of *N*-(3-dimethylaminopropyl)-*N*′-ethylcarbodiimide hydrochloride (EDC, 0.05 g, 0.2 mmol). The mixture was stirred at room temperature for 30 min. The solvent was evaporated, and the crude material was purified by column chromatography with a gradient of 50−80% ethyl acetate/hexane. The purified material was treated with 2,2,2-trifluoroacetic acid (5 mL) and refluxed for 2 h. The solvent was evaporated, and the crude material was dissolved in dichloromethane and washed with 1N NaOH. The organic layer was dried on sodium sulfate, filtered, and concentrated to give 3-(2-amino-6-*o*-tolylquinolin-3-yl)-2-methyl-*N*-(thiazol-5-ylmethyl)propanamide (0.036 g, 42% yield). ^{1}H NMR (300 MHz, chloroform-*d*) δ ppm 1.29−1.35 (m, 3 H) 2.30 (s, 3 H) 2.52−2.77 (m, 2H) 3.12 (s, 1H) 4.54 (d, J = 5.85 Hz, 2H) 5.12 (br s, 2H) 6.00−6.15 (m, 1H) 7.27−7.34 (m, 4H) 7.48 (d, J = 1.75 Hz, 1H) 7.49−7.55 (m, 1H) 7.59 (s, 1H) 7.62−7.71 (m, 2H) 8.57 (s, 1H). MS (ESI, positive ion) m/z: 417.0 (M + 1).

(*R*)-3-(2-Amino-6-*o*-tolylquinolin-3-yl)-2-methyl-*N*-(pyrazin-2-ylmethyl)propanamide (55). Chiral purification of 3-(2-(*tert*-butylamino)-6-*o*-tolylquinolin-3-yl)-2-methylpropanoic acid (prepared as in **54**) by preparative SFC: coupling of two Chiralcel OJ-H (21 mm × 25 cm × 2, 40 °C) columns; mobile phase, 88:12 (A:B), A = liquid CO_2, B = methanol (0.2% isopropylamine); 100 bar; flow rate = 70 mL/min. (*R*)-3-(2-(*tert*-Butylamino)-6-*o*-tolylquinolin-3-yl)-2-methylpropanoic acid was obtained with 100% ee.

(*R*)-3-(2-(*tert*-Butylamino)-6-*o*-tolylquinolin-3-yl)-2-methylpropanoic acid (0.10 g, 0.27 mmol) was dissolved in DMF 2 mL. Pyrazin-2-ylmethanamine (0.029 g, 0.27 mmol) and TBTU (0.10 g, 0.27 mmol) were added. The reaction mixture was stirred at room temperature for 2 h, then water was added and extracted with EtOAc three times. The combined organic layers were washed with water and brine, dried on sodium sulfate, filtered, and concentrated. The crude material was purified by prep-TLC plate with 70% ethyl acetate/hexane. The purified material was treated with 2,2,2-trifluoroacetic acid (5 mL) and refluxed for 2 h. The solvent was removed, and the residue was added dichloromethane and 1N NaOH. The organic layer was separated and dried on sodium sulfate, filtered, and concentrated. The crude product was purified by prep-TLC plate with 5% 2 M NH_3 in MeOH/dichloromethane to give (*R*)-3-(2-amino-6-*o*-tolylquinolin-3-yl)-2-methyl-*N*-(pyrazin-2-ylmethyl)propanamide (41 mg, 38% yield). ^{1}H NMR (300 MHz, chloroform-*d*) δ ppm 1.35 (d, J = 6.43 Hz, 3H) 2.30 (s, 3H) 2.54−2.89 (m, 2H) 2.98−3.28 (m, 1H) 4.53 (t, J = 4.02 Hz, 2H) 5.15 (br s, 2H) 6.58 (br s, 1H) 7.28 (s, 4H) 7.39−7.57 (m, 2H) 7.57−7.78 (m, 2H) 8.29 (s, 1H) 8.39 (s, 1H) 8.51 (s, 1H). MS (ESI, positive ion) m/z: 412.0 (M + 1).

(*R*)-3-(2-Amino-6-*o*-tolylquinolin-3-yl)-2-methyl-*N*-((tetrahydro-2*H*-pyran-4-yl)methyl)propanamide (56). Using (tetrahydro-2*H*-pyran-4-yl)methanamine and following the procedure used to prepare **55** gave **56**. ^{1}H NMR (400 MHz, chloroform-*d*) δ ppm 1.00−1.17 (m, 3H) 1.23−1.30 (m, 1H) 1.33 (d, J = 6.65 Hz, 3H) 1.41−1.51 (m, 1H) 2.30 (s, 3H) 2.54−2.64 (m, 1H) 2.64−2.72 (m, 1H) 2.81−2.92 (m, 1H) 3.01 (m, 1H) 3.05−3.22 (m, 3H) 3.66−3.74 (m, 1H) 3.74−3.83 (m, 1H) 5.18 (br s, 2H) 5.49 (br s, 1H) 7.26−7.34 (m, 4H) 7.48−7.54 (m, 2H) 7.65 (d, J = 9.00 Hz, 1H) 7.70 (s, 1H). MS (ESI, positive ion) m/z: 418.0 (M + 1).

(*R*)-3-(2-Amino-6-*o*-tolylquinolin-3-yl)-*N*-((*R*)-2,2-dimethyltetrahydro-2*H*-pyran-4-yl)-2-methylpropanamide (57). A 20 mL vial was charged with (*R*)-3-(2-(*tert*-butylamino)-6-*o*-tolylquinolin-3-yl)-2-methylpropanoic acid (0.13 g, 0.33 mmol, prepared as in **55**), 3,3-dimethylcyclohexanaminium chloride (0.068 g, 0.42 mmol), TBTU (0.13 g, 0.42 mmol), and 2 mL of NMP. To the resulting mixture was added *N*-ethyl-*N*-isopropylpropan-2-amine (0.15 mL, 0.83 mmol). After stirring at room temperature for 2 h, the mixture was diluted with water and extracted with EtOAc. The combined organic layers were dried on sodium sulfate, filtered, and concentrated. The resulting two diastereomers were separated and purified via column chromatography with a gradient of 0−50% ethyl acetate/hexane to give (*R*)-3-(2-amino-6-*o*-tolylquinolin-3-yl)-*N*-((*R*)-2,2-dimethyltetrahydro-2*H*-pyran-4-yl)-2-methylpropanamide and (*R*)-3-(2-amino-6-o-tolylquinolin-3-yl)-*N*-((*S*)-2,2-dimethyltetrahydro-2*H*-pyran-4-yl)-2-methylpropanamide.
These two compounds were treated individually with 2,2,2-trifluoroacetic acid (3 mL) and refluxed for 2 h. The solvent was removed and to the residue was added dichromethane and 1N NaOH. The organic layer was separated and dried on sodium sulfate, filtered, and concentrated. The crude product was purified by column chromatography on silica gel with a gradient of 0−5% 2 M NH_3 in MeOH/dichloromethane to give (*R*)-3-(2-amino-6-*o*-tolylquinolin-3-yl)-*N*-((*S*)-2,2-dimethyltetrahydro-2*H*-pyran-4-yl)-2-methylpropanamide and (*R*)-3-(2-amino-6-*o*-tolylquinolin-3-yl)-*N*-((*R*)-2,2-dimethyltetrahydro-2*H*-pyran-4-yl)-2-methylpropanamide (is consistent with the determined co-crystal structure). ^{1}H NMR (400 MHz, methanol-d_4) δ 8.16 (br s, 1H), 7.84−7.66 (m, 4H), 7.36−7.16 (m, 4H), 3.71 (br s, 1H), 2.90−2.62 (m, 2H), 2.26 (m, 3H), 1.84−1.60 (m, 1H), 1.58−1.35 (m, 3H), 1.35−1.17 (m, 5H), 1.06−0.83 (m, 6H). MS (ESI, positive ion) m/z: 432 (M + 1).

(*R*)-3-(2-Amino-6-(3-methylpyridin-2-yl)quinolin-3-yl)-*N*-(3,3-dimethylbutyl)-2-methylpropanamide (58). TBTU (1.2 g, 3.7 mmol) was added to 3-(2-(4-methoxybenzylamino)-6-bromoquinolin-3-yl)-2-methylacrylic acid (1.2 g, 2.8 mmol, prepared as in **53**), 3,3-dimethylbutylamine (1.1 mL, 8.4 mmol), and *N*,*N*-diisopropylethylamine (2.0 mL, 11 mmol) in NMP (10 mL), and the reaction was stirred for 1 h. The reaction mixture was then poured into a vigorously stirred solution of saturated aqueous sodium bicarbonate.

After 30 min, ethyl acetate was added. The layers were separated, and the aqueous layer was extracted with ethyl acetate. The combined organic layers were washed with water, brine, dried over sodium sulfate, filtered, and concentrated to afford 3-(6-bromo-2-(4-methoxybenzylamino)quinolin-3-yl)-*N*-(3,3-dimethylbutyl)-2-methylacrylamide, which was used without further purification.

Dichloro(1,1′-bis(diphenylphosphino)ferrocene) palladium(II) (0.096 g, 0.12 mmol) was added to a solution of 3-(6-bromo-2-(4-methoxybenzylamino)quinolin-3-yl)-*N*-(3,3-dimethylbutyl)-2-methylacrylamide (1.2 g, 2.4 mmol), potassium acetate (0.69 g, 7.1 mmol), and 4,4,5,5-tetramethyl-2-(4,4,5,5-tetramethyl-1,3,2-dioxaborolan-2-yl)-1,3,2-dioxaborolane (0.72 g, 2.8 mmol) in dioxane (20 mL, degassed with nitrogen). The reaction mixture was heated at 85 °C for 4 h, and then it was cooled and concentrated. The crude product was diluted with ethyl acetate and filtered. The filtrate was concentrated to afford 3-(2-(4-methoxybenzylamino)-6-(4,4,5,5-tetramethyl-1,3,2-dioxaborolan-2-yl)quinolin-3-yl)-*N*-(3,3-dimethylbutyl)-2-methylacrylamide, which was used for the next reaction without further purification.

Bis(4-(di-*tert*-butylphosphino)-*N*,*N*-dimethylbenzenamine) dichloropalladium(II) (0.041 g, 0.058 mmol) was added to a degassed solution of 3-(2-(4-methoxybenzylamino)-6-(4,4,5,5-tetramethyl-1,3,2-dioxaborolan-2-yl)quinolin-3-yl)-*N*-(3,3-dimethylbutyl)-2-methylacrylamide (0.60 g, 1.1 mmol), potassium acetate (0.211 g, 2.2 mmol), and 2-bromo-3-methylpyridine (0.18 mL, 1.6 mmol) in EtOH (12 mL) and water (2 mL). The resulting solution was refluxed for 12 h. Then the reaction mixture was cooled and partitioned between dichloromethane and 9:1 saturated ammonium chloride/ammonium hydroxide aqueous solution. The aqueous layer was extracted with dichloromethane, and the combined organics were washed with a 9:1 saturated ammonium chloride/ammonium hydroxide solution, water, brine, dried over sodium sulfate, filtered, and concentrated. The crude product was purified by silica gel column chromatography eluted with 1:1 ethyl acetate/hexane to afford 3-(2-(4-methoxybenzylamino)-6-(3-methylpyridin-2-yl)quinolin-3-yl)-*N*-(3,3-dimethylbutyl)-2-methylacrylamide. (0.034 g, 61% yield).

Palladium on carbon (0.71 g, 0.67 mmol) was added to a solution of 3-(2-(4-methoxybenzylamino)-6-(3-methylpyridin-2-yl)quinolin-3-yl)-*N*-(3,3-dimethylbutyl)-2-methylacrylamide (0.35 g, 0.67 mmol) in EtOH (6 mL). The flask was degassed with hydrogen gas and then stirred under a balloon of hydrogen 12 h. The reaction was filtered through a pad of Celite and washed with ethanol and ethyl acetate. The filtrate was concentrated to afford 3-(2-(4-methoxybenzylamino)-6-(3-methylpyridin-2-yl)quinolin-3-yl)-*N*-(3,3-dimethylbutyl)-2-methylpropanamide, which was used without further purification.

TFA (6.0 mL, 78 mmol) was added to 3-(2-(4-methoxybenzylamino)-6-(3-methylpyridin-2-yl)quinolin-3-yl)-*N*-(3,3-dimethylbutyl)-2-methylpropanamide (0.30 g, 0.57 mmol), and the reaction was heated to 65 °C. After 5 h, the reaction was concentrated and the crude material dissolved in dichloromethane. The organic layer was washed with 1N NaOH, and the aqueous layer was again extracted with dichloromethane. The combined organic layers were washed with brine, dried over sodium sulfate, and concentrated. The crude product was purified by reverse phase HPLC to afford 3-(2-amino-6-(3-methylpyridin-2-yl)quinolin-3-yl)-*N*-(3,3-dimethylbutyl)-2-methylpropanamide. (0.20 g, 76% yield over two steps)

Chiral purificaton of the racemic material via preparative SFC afforded (*S*)- and (*R*)-3-(2-amino-6-(3-methylpyridin-2-yl)quinolin-3-yl)-*N*-(3,3-dimethylbutyl)-2-methylpropanamide: Chiralcel OJ-H (4.6 mm × 15 cm, 40 °C) column; mobile phase 12% 2-propanol (0.2% DEA)/CO_2; 100 bar; flow rate = 4 mL/min; 252 nm. The resulting enantiomers have ee values of >99%, respectively.

^{1}H NMR (400 MHz, chloroform-*d*) δ ppm 0.81 (s, 9H) 1.17−1.27 (m, 3H) 1.23 (d, J = 8 Hz, 3H) 2.39 (s, 3H) 2.48−2.55 (m, 1H) 2.59−2.64 (m, 1H) 3.04−3.23 (m, 3H) 5.34 (br s, 2H) 5.62−5.64 (m, 1H) 7.16 (dd, J = 4 Hz, J = 8 Hz, 1H) 7.58 (d, J = 8 Hz, 1H) 7.67−7.71 (m, 3H) 7.73 (s, 1H) 8.52 (d, J = 4 Hz, 1H). MS (ESI, positive ion) m/z: 405 (M + 1).

(*R*)-3-(2-Amino-6-(3-chloropyridin-2-yl)quinolin-3-yl)-*N*-(3,3-dimethylbutyl)-2-methylpropanamide (59). Bis(4-(di-*tert*-butylphosphino)-*N*,*N*-dimethylbenzenamine) dichloropalladium(II) (0.038 g, 0.054 mmol) was added to a degassed solution of 3-(2-(4-methoxybenzylamino)-6-(4,4,5,5-tetramethyl-1,3,2-dioxaborolan-2-yl)quinolin-3-yl)-*N*-(3,3-dimethylbutyl)-2-methylacrylamide (0.60 g, 1.1 mmol, prepared as in **58**, potassium acetate (0.211 g, 2.15 mmol), 2-bromo-3-chloropyridine (0.31 g, 1.61 mmol) in EtOH (12 mL), and water (2 mL). The reaction mixture was refluxed for 12 h. Then it was cooled and partitioned between dichloromethane and 9:1 saturated ammonium chloride/ammonium hydroxide. The aqueous layer was extracted with dichloromethane. The combined organic layers were washed with a 9:1 saturated ammonium chloride/ammonium hydroxide solution, water, brine, dried over sodium sulfate, filtered, and concentrated. The crude material was purified by column chromatography eluted with 1.5:1 hexane/ethyl acetate to afford 3-(2-(4-methoxybenzylamino)-6-(3-chloropyridin-2-yl)quinolin-3-yl)-*N*-(3,3-dimethylbutyl)-2-methylacrylamide (0.49 g, 84% yield).

Platinum on carbon (5%), (0.70 g, 0.18 mmol) was added to a degassed solution of 3-(2-(4-methoxybenzylamino)-6-(3-chloropyridin-2-yl)quinolin-3-yl)-*N*-(3,3-dimethylbutyl)-2-methylacrylamide (0.49 g, 0.9 mmol) in EtOH (10 mL). The flask was degassed with hydrogen gas and then stirred under a balloon of hydrogen 12 h. The reaction was filtered through Celite and washed with ethanol and ethyl acetate. The filtrate was concentrated to afford 3-(2-(4-methoxybenzylamino)-6-(3-chloropyridin-2-yl)quinolin-3-yl)-*N*-(3,3-dimethylbutyl)-2-methylpropanamide, which was used directly for the next step without further purification.

TFA (5.0 mL, 65 mmol) was added to 3-(2-(4-methoxybenzylamino)-6-(3-chloropyridin-2-yl)quinolin-3-yl)-*N*-(3,3-dimethylbutyl)-2-methylpropanamide (0.30 g, 0.57 mmol), and the reaction was heated to 65 °C. After 6 h, the reaction was concentrated and was purified by reverse phase HPLC to afford 3-(2-amino-6-(3-chloropyridin-2-yl)quinolin-3-yl)-*N*-(3,3-dimethylbutyl)-2-methylpropanamide (0.082 g, 21% yield over two steps).

Chiral purificaton of the racemic material via preparative SFC afforded (*S*)- and (*R*)-3-(2-amino-6-(3-chloropyridin-2-yl)quinolin-3-yl)-*N*-(3,3-dimethylbutyl)-2-methylpropanamide: Chiralpak AD-H (2 cm × 15 cm, 40 °C) column; mobile phase 20% methanol (0.1% DEA)/CO_2; 100 bar; flow rate = 70 mL/min, 220 nm. The resulting enantiomers have ee values of >99%, respectively.

^{1}H NMR (400 MHz, chloroform-*d*) δ ppm 0.83 (s, 9H) 1.19−1.23 (m, 2H) 1.28 (d, J = 8 Hz, 3H) 2.48−2.55 (m, 1H) 2.63−2.66 (m, 1H) 3.08−3.20 (m, 3H) 5.33 (br s, 2H) 5.35−5.41 (m, 1H) 7.21 (dd, J = 4 Hz, J = 8 Hz, 1H) 7.69 (d, J = 8 Hz, 1H) 7.73 (s, 1H) 7.81 (d, J = 8 Hz, 1H) 7.91 (dd, J = 4 Hz, J = 8 Hz, 1H) 8.00 (s, 1H) 8.61 (d, J = 4 Hz, 1H). MS (ESI, positive ion) m/z: 425 (M + 1).

3-(2-Amino-6-(3-methoxypyridin-2-yl)quinolin-3-yl)-*N*-(3,3-dimethylbutyl)-2-methylpropanamide (60). Using 2-iodonicotinonitrile and following the procedures used to prepare **58** gave **60**. ^{1}H NMR (300 MHz, chloroform-*d*) δ ppm 0.83 (s, 9H) 1.08−1.37 (m, 6H) 2.44−2.58 (m, 1H) 2.58−2.73 (m, 1H) 3.15 (br s, 2H) 3.90 (s, 3H) 5.27−5.49 (m, 1H) 6.08−6.32 (m, 1H) 7.17−7.25 (m, 1H) 7.30 (s, 1H) 7.73 (s, 1H) 7.77 (s, 1H) 8.19 (s, 2H) 8.33 (br s, 1H). MS (ESI, positive ion) m/z: 416.0 (M + 1).

3-(2-Amino-6-(3-cyanopyridin-2-yl)quinolin-3-yl)-*N*-(3,3-dimethylbutyl)-2-methylpropanamide (61). Using 2-iodo-3-methoxypyridine and following the procedures used to prepare **58** gave **61**. ^{1}H NMR (300 MHz, chloroform-*d*) δ ppm 0.84 (s, 9H) 1.11−1.41 (m, 6H) 2.42−2.59 (m, 1H) 2.59−2.74 (m, 1H) 3.18 (d, J = 4.38 Hz, 2H) 5.32−5.49 (m, 1H) 5.57−5.85 (m, 1H) 7.31−7.45 (m, 1H)

7.69−7.86 (m, 2H) 8.02−8.15 (m, 2H) 8.23 (s, 1H) 8.82−8.99 (m, 1H). MS (ESI, positive ion) *m/z*: 421.0 (M + 1).

3-(6-(2-Acetylphenyl)-2-aminoquinolin-3-yl)-*N*-(3,3-dimethylbutyl)-2-methylpropanamide (62). Using 1-(2-bromophenyl)ethanone and following the procedures used to prepare **58** gave **62**. ^{1}H NMR (300 MHz, chloroform-*d*) δ ppm 0.77 (s, 9H) 1.04−1.36 (m, 6H) 1.57−1.83 (m, 1H) 1.93 (s, 3H) 2.38−2.52 (m, 1H) 2.52−2.65 (m, 1H) 2.95−3.22 (m, 2H) 5.36 (br s, 2H) 7.28−7.55 (m, 6H) 7.56−7.71 (m, 2H). MS (ESI, positive ion) *m/z*: 432.1 (M + 1).

■ ASSOCIATED CONTENT

Supporting Information. X-ray crystallographic data (collection details, refinement statistics). This material is available free of charge via the Internet at http://pubs.acs.org.

Accession Codes

[†]New protein/ligand coordinates have been deposited in the PDB with IDs of 3RSV, 3RSX, 3RTH, 3RTM, 3RTN, 3RU1, and 3RVI.

■ AUTHOR INFORMATION

Corresponding Author

*Phone: 805-447-3543. Fax: 805-480-3016. E-mail: yuanc@amgen.com (Y.C.) or tjudd@amgen.com (T.C.J.).

Present Addresses

[▽]Envoy Therapeutics, Jupiter, Florida, United States

■ ACKNOWLEDGMENT

We thank Kyung Gahm, Sonia Hua, and Wesley Barnhart for chiral separation. We also would like to acknowledge the contributions of Dr. Leszek Poppe in the development of the ^{19}F-based enzymatic assay described in this paper. The Advanced Light Source is supported by the U.S. Department of Energy under contract no. DE-AC02-05CH11231.

■ ABBREVIATIONS USED

BACE, beta-site APP-Cleaving Enzyme; AD, Alzheimer's disease; Aβ, β-amyloid; APP, amyloid precursor protein; sAPPβ, soluble amyloid precursor protein-betaSAR, structure−activity relationship; CNS, central nervous system; Pgp, P-glycoprotein; LE, ligand efficiency; PSA, polar surface area; CSF, cerebrospinal fluid; ER, efflux ratio; HTS, high throughput screening; SPR, surface plasmon resonance; PD, pharmacodynamic; K_d, dissociation constant; ee, enantiomeric excess; NMP, *N*-Methyl-2-pyrrolidone; DMF, *N*,*N*-dimethylformamide; TBTU, *O*-(Benzotriazol-1-yl)-*N*,*N*,*N*′,*N*′-tetra-methyluronium tetra-fluoroborate; PS-PPh$_3$-Pd, polystyrene triphenylphosphine palladium(0); EDC, 1-Ethyl-3-(3-dimethylaminopropyl)carbodiimide hydrochloride; DMSO, dimethyl sulfoxide

■ ADDITIONAL NOTE

[a] Graphics were created with (i) The PyMOL Molecular Graphics System, version 1.3, Schrödinger, LLC and (ii) MOLCAD as implemented in Sybyl version 8.0, (Tripos International, St. Louis MO, USA) and annotated with Adobe Photoshop CS2, version 9.0.2 for Windows, Adobe, Inc.

■ REFERENCES

(1) Querfurth, H. W.; LaFeral, F. M. Mechanisms of Disease: Alzheimer's disease. *N. Engl. J. Med.* **2010**, *362*, 329–344.

(2) (a) Hardy, J.; Selkoe, D. J. The amyloid hypothesis of Alzheimer's disease: progress and problems on the road to therapeutics. *Science* **2002**, *297*, 353–356. (b) De Strooper, B.; Vasar, R.; Golde, T. The secretases: enzymes with therapeutic potential in Alzheimer's disease. *Nature Rev. Neurol.* **2010**, *6*, 99–107.

(3) Vassar, R.; Bennett, B. D.; Babu-Khan, S.; Kahn, S.; Mendiaz, E. A.; Denis, P.; Teplow, D. B.; Ross, S.; Amarante, P.; Loeloff, R.; Luo, Y.; Fisher, S.; Fuller, J.; Edenson, S.; Lile, J.; Jarosinski, M. A.; Biere, A. L.; Curran, E.; Burgess, T.; Louis, J. C. Beta-secretase cleavage of Alzheimer's amyloid precursor protein by the transmembrane aspartic protease BACE. *Science* **1999**, *286*, 735–741.

(4) Vassar, R.; Kovacs, D. M.; Yan, R.; Wong, P. C. The β-secretase enzyme in health and Alzheimer's disease: regulation, cell biology, function, and therapeutic potential. *J. Neurosci.* **2009**, *29*, 12787–12794.

(5) Younkin, S. G. The role of A beta 42 in Alzheimer's disease. *J. Physiol. (Paris)* **1998**, *92*, 289–292.

(6) Citron, M. Alzheimer's disease: strategies for disease modification. *Nature Rev.* **2010**, *9*, 387–398.

(7) (a) Luo, Y.; Bolon, B.; Kahn, S.; Bennett, B. D.; Babu-Khan, S.; Denis, P.; Fan, W.; Kha, H.; Zhang, J.; Gong, Y.; Martin, L.; Louis, J.-C.; Yan, Q.; Richards, W. G.; Citron, M.; Vassar, R. Mice deficient in BACE1, the Alzheimer's beta-secretase, have normal phenotype and abolished beta-amyloid generation. *Nature Neurosci.* **2001**, *4*, 231–232. (b) Roberds, S. L.; Anderson, J.; Basi, G.; Bienkowski, M. J.; Branstetter, D. G.; Chen, K. S.; Freedman, S. B.; Frigon, N. L.; Games, D.; Hu, K.; Johnson-Wood, K.; Kappenman, K. E.; Kawabe, T. T.; Kola, I.; Kuehn, R.; Lee, M.; Liu, W.; Motter, R.; Nichols, N. F.; Power, M.; Robertson, D. W.; Schenk, D.; Schoor, M.; Shopp, G. M.; Shuck, M. E.; Sinha, S.; Svensson, K. A.; Tatsuno, G.; Tintrup, H.; Wijsman, J.; Wright, S.; McConlogue, L. BACE knockout mice are healthy despite lacking the primary beta-secretase activity in brain: implications for Alzheimer's disease therapeutics. *Hum. Mol. Genet.* **2001**, *10*, 1317–1324.

(8) (a) Ohno, M.; Sametsky, E. A.; Younkin, L. H.; Oakley, H.; Younkin, S. G.; Citron, M.; Vassar, R.; Disterhoft, J. F. BACE1 deficiency rescues memory deficits and cholinergic dysfunction in a mouse model of Alzheimer's disease. *Neuron* **2004**, *41*, 27–33. (b) McConlogue, L.; Buttini, M.; Anderson, J. P.; Brigham, E. F.; Chen, K. S.; Freedman, S. B.; Games, D.; Johnson-Wood, K.; Lee, M.; Zeller, M.; Liu, W.; Motter, R.; Sinha, S. Partial reduction of BACE1 has dramatic effects on Alzheimer plaque and synaptic pathology in APP transgenic mice. *J. Biol. Chem.* **2007**, *282*, 26326–26334.

(9) (a) Hitchcock, S. A.; Pennington, L. D. Structure−brain exposure relationships. *J. Med. Chem.* **2006**, *49*, 7559–7583. (b) Clark, D. E. Rapid calculation of polar molecular surface area and its application to the prediction of transport phenomena. 2. Prediction of blood−brain barrier phenetration. *J. Pharm. Sci.* **1999**, *88*, 815–821. (c) Lipinski, C. A.; Lombardo, F.; Dominy, B. W.; Feeney, P. J. Experimental and computational approaches to estimate solubility and permeability in drug discovery and development settings. *Adv. Drug Delivery Rev.* **2001**, *46*, 3–26.

(10) Zhong, W.; Hitchcock, S. A.; Albrecht, B. K.; Bartberger, M.; Brown, J.; Brown, R.; Chaffee, S. C.; Cheng, Y.; Croghan, M.; Graceffa, R.; Harried, S.; Hickman, D.; Horne, D.; Hungate, R.; Judd, T.; Kaller, M.; Kreiman, C.; La, D.; Lopez, P.; Masse, C. E.; Monenschein, H.; Nguyen, T.; Nixey, T.; Patel, V. F.; Pennington, L.; Weiss, M.; Xue, Q.; Yang, B. Preparation of 2-hydroxy-1,3-diaminoalkanes including spiro substituted chroman derivatives as β-secretase modulators and their use for treatment Alzheimer's disease and related condition. Patent WO2007061670, 2007.

(11) Ghosh, A. K.; Kumaragurubaran, N.; Hong, L.; Kulkarni, S. S.; Xu, X.; Chang, W.; Weerasena, V.; Turner, R.; Koelsch, G.; Bilcer, G.; Tang, J. Design, synthesis, and X-ray structure of potent memapsin 2 (β-secretase) inhibitors with isophthalamide derivatives as the P2-P3-ligands. *J. Med. Chem.* **2007**, *50*, 2399–2407.

(12) Maillard, M. C.; Hom, R. K.; Benson, T. E.; Moon, J. B.; Mamo, S.; Bienkowski, M.; Tomasselli, A. G.; Woods, D. D.; Prince, D. B.; Paddock, D. J.; Emmons, T. L.; Tucker, J. A.; Dappen, M. S.; Brogley, L.; Thorsett, E. D.; Jewett, N.; Sinha, S.; John, V. Design, synthesis, and crystal structure of hydroxyethyl secondary amine-based peptidomimetic inhibitors of human β-secretase. *J. Med. Chem.* **2007**, *50*, 776–781.

(13) Ghosh, A. K.; Kumaragurubaran, N.; Tang, J. Recent developments of structure-based β-secretase inhibitors for Alzheimer's disease. *Curr. Top. Med. Chem.* **2005**, *5*, 1609–1622.

(14) Silvestri, R. Boom in the development of non-peptidic beta-secretase (BACE1) inhibitors for the treatment of Alzheimer's disease. *Med. Res. Rev.* **2009**, *29*, 295–338.

(15) Hamada, Y.; Kiso, Y. Recent progress in the drug discovery of non-peptidic BACE1 inhibitors. *Expert Opin. Drug Discovery* **2009**, *4*, 391–416and references therein.

(16) (a) Malamas, M. S.; Erdei, J.; Gunawan, I.; Turner, J.; Hu, Y.; Wagner, E.; Fan, K.; Chopra, R.; Olland, A.; Bard, J.; Jocobsen, S.; Magolda, R. L.; Pangalos, M.; Robichaud, A. J. Design and synthesis of 5,5′-disubstituted aminohydantoins as potent and selective human β-secretase (BACE1) inhibitor. *J. Med. Chem.* **2010**, *53*, 1146–1158. (b) Malamas, M. S.; Erdei, J.; Gunawan, I.; Barnes, K.; Johnson, M.; Hui, Y.; Turner, J.; Hu, Y.; Wagner, E.; Fan, K.; Olland, A.; Bard, J.; Robichaud, A. J. Aminoimidazoles as potent and selective human β-secretase (BACE1) inhibitors. *J. Med. Chem.* **2009**, *52*, 6314–6323.

(17) Zhu, Z.; Sun, Z.-Y.; Ye, Y.; Voigt, J.; Strickland, C.; Smith, E. M.; Cumming, J.; Wang, L.; Wong, J.; Wang, Y.-S.; Wyss, D. F.; Chen, X.; Kuvelkar, R.; Kennedy, M. E.; Favreau, L.; Parker, E.; McKittrick, B. A.; Stamford, A.; Czarniecki, M.; Greenlee, W.; Hunter, J. C. Discovery of cyclic acylguanidines as highly potent and selective β-site amyloid cleaving enzyme (BACE) inhibitors: Part I: Inhibitor design and validation. *J. Med. Chem.* **2010**, *53*, 951–965.

(18) Baxter, E. W.; Conway, K. A.; Kennis, L.; Bischoff, F.; Mercken, M. H.; De Winter, H. L.; Reynolds, C. H.; Tounge, B. A.; Luo, C.; Scott, M. K.; Huang, Y.; Braeken, M.; Pieters, S. M. A.; Berthelot, D. J. C.; Masure, S.; Bruinzeel, W. D.; Jordan, A. D.; Parker, M. H.; Boyd, R. E.; Qu, J.; Alexander, R. S.; Brenneman, D. E.; Reitz, A. B. 2-Amino-3,4-dihydroquinazolines as inhibitors of BACE-1 (β-site APP cleaving enzyme): use of structure based design to convert a micromolar hit into a nanomolar lead. *J. Med. Chem.* **2007**, *50*, 4261–4264.

(19) Orita, M.; Warizaya, M.; Amano, Y.; Ohno, K.; Niimi, T. Advances in fragment-based drug discovery platforms. *Curr. Opin. Pharmacol.* **2009**, *9*, 615–621.

(20) Eitner, K.; Koch, U. From fragment screening to potent binders: strategies for fragment-to-lead evolution. *Mini-Rev. Med. Chem.* **2009**, *9*, 956–961.

(21) Chessari, G.; Woodhead, A. J. From fragment to clinical candidate-a historical perspective. *Drug Discovery Today* **2009**, *14*, 668–675.

(22) Fattori, D.; Squarcia, A.; Bartoli, S. Fragment-based approach to drug lead discovery: overview and advances in various techniques. *Drugs R&D* **2008**, *9*, 217–227.

(23) Wyss, D. F.; Eaton, H. L. Fragment-based approaches to lead discovery. *Front. Drug Des. Discovery* **2007**, *3*, 171–202.

(24) Reynolds, C. H.; Tounge, B. A.; Bembenek, S. D. Ligand binding efficiency: trends, physical basis, and implications. *J. Med. Chem.* **2008**, *51*, 2432–2438.

(25) Abad-Zapatero, C. Ligand efficiency indices for effective drug discovery. *Expert Opin. Drug Discovery* **2007**, *2*, 469–488.

(26) Wang, Y.-S.; Strickland, C.; Voigt, J. H.; Kennedy, M. E.; Beyer, B. M.; Senior, M. M.; Smith, E. M.; Nechuta, T. L.; Madison, V. S.; Czarniecki, M.; McKittrick, B. A.; Stamford, A. W.; Parker, E. M.; Hunter, J. C.; Greenlee, W. J.; Wyss, D. F. Application of Fragment-Based NMR Screening, X-ray Crystallography, Structure-Based Design, and Focused Chemical Library Design to Identify Novel μM Leads for the Development of nM BACE-1 (β-Site APP Cleaving Enzyme 1) Inhibitors. *J. Med. Chem.* **2010**, *53*, 942–950.

(27) Godemann, R.; Madden, J.; Kramer, J.; Smith, M.; Fritz, U.; Hesterkamp, T.; Barker, J.; Hoeppner, S.; Hallett, D.; Cesura, A.; Ebneth, A.; Kemp, J. Fragment-based discovery of BACE1 inhibitors using functional assays. *Biochemistry* **2009**, *48*, 10743–10751.

(28) Yang, W.; Fucini, R. V.; Fahr, B. T.; Randal, M.; Lind, K. E.; Lam, M. B.; Lu, W.; Lu, Y.; Cary, D. R.; Romanowski, M. J.; Colussi, D.; Pietrak, B.; Allison, T. J.; Munshi, S. K.; Penny, D. M.; Pham, P.; Sun, J.; Thomas, A. E.; Wilkinson, J. M.; Jacobs, J. W.; McDowell, R. S.; Ballinger, M. D. Fragment-Based Discovery of Nonpeptidic BACE-1 Inhibitors Using Tethering. *Biochemistry* **2009**, *48*, 4488–4496.

(29) (a) Albert, J. S.; Blomberg, N.; Breeze, A. L.; Brown, A. J. H.; Burrows, J. N.; Edwards, P. D.; Folmer, R. H. A.; Geschwindner, S.; Griffen, E. J.; Kenny, P. W.; Nowak, T.; Olsson, L.-L.; Sanganee, H.; Shapiro, A. B. An integrated approach to fragment-based lead generation: philosophy, strategy and case studies from AstraZeneca's drug discovery programs. *Curr. Top. Med. Chem.* **2007**, *7*, 1600–1629. (b) Edwards, P. D.; Albert, J. S.; Sylvester, M.; Aharony, D.; Andisik, D.; Callaghan, O.; Campbell, J. B.; Carr, R. A.; Chessari, G.; Congreve, M.; Frederickson, M.; Folmer, R. H. A.; Geschwindner, S.; Koether, G.; Kolmodin, K.; Krumrine, J.; Mauger, R. C.; Murray, C. W.; Olsson, L.-L.; Patel, S.; Spear, N.; Tian, G. Application of fragment-based lead generation to the discovery of novel, cyclic amidine β-secretase inhibitors with nanomolar potency, cellular activity, and high ligand efficiency. *J. Med. Chem.* **2007**, *50*, 5912–5925. (c) Geschwindner, S.; Olsson, L.-L.; Albert, J. S.; Deinum, J.; Edwards, P. D.; de Beer, T.; Folmer, R. H. A. Discovery of a Novel Warhead against β-Secretase through Fragment-Based Lead Generation. *J. Med. Chem.* **2007**, *50*, 5903–5911.

(30) Murray, C. W.; Callaghan, O.; Chessari, G.; Cleasby, A.; Congreve, M.; Frederickson, M.; Hartshorn, M. J.; McMenamin, R.; Patel, S.; Wallis, N. Application of fragment screening by X-ray crystallography to β-secretase. *J. Med. Chem.* **2007**, *50*, 1116–1123.

(31) Congreve, M.; Aharony, D.; Albert, J.; Callaghan, O.; Campbell, J.; Carr, R. A. E.; Chessari, G.; Cowan, S.; Edwards, P. D.; Frederickson, M.; McMenamin, R.; Murray, C. W.; Patel, S.; Wallis, N. Application of fragment screening by X-ray crystallography to the discovery of aminopyridines as inhibitors of β-secretase. *J. Med. Chem.* **2007**, *50*, 1124–1132.

(32) (a) Huber, W.; Mueller, F. Biomolecular interaction analysis in drug discovery using surface plasmon resonance technology. *Curr. Pharm. Des.* **2006**, *12*, 2999–4021. (b) Huber, W. A new strategy for improved secondary screening and lead optimization using high-resolution SPR characterization of compound-target interactions. *J. Mol. Recognit.* **2005**, *18*, 273–281.

(33) Meth-Cohn, O.; Narine, B.; Tarnowski, B. A versatile new synthesis of quinolines and related fused pyridines. Part 5. The synthesis of 2-chloroquinoline-3-carboxaldehydes. *J. Chem. Soc., Perkin Trans. 1* **1981**, *5*, 1520–1530.

(34) Wang, Q.; Rager, J. D.; Weinstein, K.; Kardos, P. S.; Dobson, G. L.; Li, J.; Hidalgo, I. J. Evaluation of the MDR-MECK cell line as a permeability screen for the blood−brain barrier. *Int. J. Pharm.* **2005**, *288*, 349–359.

(35) Liu, X.; Chen, C. Strategies to optimize brain penetration in drug discovery. *Curr. Opin. Drug Discovery Dev.* **2005**, *8*, 505–512.

(36) Wong, G. T.; Manfra, D.; Poulet, F. M.; Zhang, Q.; Josien, H.; Bara, T.; Engstrom, L.; Pinzon-Ortiz, M.; Fine, J. S.; Lee, H. J.; Zhang, L.; Higgins, G. A.; Parker, E. M. Chronic treatement with the γ-secretase inhibitor LY-411,575 inhibits β-amyloid peptide production and alters lymphopoiesis and intestinal cell differentiation. *J. Biol. Chem.* **2004**, *279*, 12876–12882.

(37) Turner, R. T., III; Koelsch, G.; Hong, L.; Castanheira, P.; Ghosh, A.; Tang, J. Subsite specificity of memapsin (β-secretase): implications for inhibitor design. *Biochemistry* **2001**, *40*, 10001–10006.

(38) Haniu, M.; Denis, P.; Young, Y.; Mendiaz, E. A.; Fuller, J.; Hui, J. O.; Bennett, B. D.; Kahn, S.; Ross, S.; Burgess, T. Characterization of Alzheimer's beta-secretase protein BACE. A pepsin family member with unusual properties. *J. Biol. Chem.* **2000**, *275*, 21099–21106.

(39) Schinkel, A. H.; Wagenaar, E.; van Deemter, L.; Mol, C. A. A. M.; Borst, P. Absence of the mdr1a P-glycoprotein in mice affects tissue distribution and pharmacokinetics of dexamethasone, digoxin, and cyclosporin A. *J. Clin. Invest.* **1995**, *96*, 1698–1705.

(40) Booth-Genthe, C. L.; Louie, S. W.; Carlini, E. J.; Li, B.; Leake, B. F.; Eisenhandler, R.; Hochman, J. H.; Mei, Q.; Kim, R. B.; Rushmore, T. H.; Yamazaki, M. Development and characterization of LLC-PK1 cells containing Sprague−Dawley rat *Abcb*1a (*Mdr*1a): Comparison of rat P-glycoprotein transport to human and mouse. *J. Pharmacol. Toxicol. Methods* **2006**, *54*, 78–89.

(41) Patel, S.; Vuillard, L.; Cleasby, A.; Murray, C. W.; Yon, J. Apo and inhibitor complex structures of BACE (beta-secretase). *J. Mol. Biol.* **2004**, *343*, 407–416.

(42) Otwinowski, Z.; Minor, W. Processing of X-ray diffraction data collected in oscillation mode. *Methods Enzymol.* **1997**, *276*, 307–326.

(43) McCoy, A. J.; Grosse-Kunstleve, R. W.; Adams, P. D.; Winn, M. D.; Storoni, L. C.; Read, R. J. Phaser crystallographic software. *J. Appl. Crystallogr.* **2007**, *40*, 658–674.

(44) Murshudov, G. N.; Vagin, A. A.; Dodson, E. J. Refinement of macromolecular structures by the maximum-likelihood method. *Acta Crystallogr., Sect. D: Biol. Crystallogr.* **1997**, *D53*, 240–255.

(45) Emsley, P.; Cowtan, K. Coot: model-building tools for molecular graphics. *Acta Crystallogr., Sect. D: Biol. Crystallogr.* **2004**, *D60*, 2126–2132.